Effect of aluminum oxyhydroxide coatings on the performance of limestone drains

Sheyla Bethsy Palomino Ore

Thesis submitted to the faculty of the Virginia Polytechnic Institute and State University
in partial fulfillment of the requirements for the degree of

Master of Science
In
Geosciences

Madeline Schreiber
John Chermak
J. Donald Rimstidt
Robert Seal

April 27, 2018
Blacksburg, Virginia

Keywords: Acid mine drainage, limestone drains, aluminum, oxyhydroxide, coatings

Effect of aluminum oxyhydroxide coatings on the performance of limestone drains

Sheyla Bethsy Palomino Ore

ACADEMIC ABSTRACT

Neutralization by limestone is a common treatment for acid mine drainage (AMD). The effectiveness of using limestone to treat AMD can be reduced by aluminum (Al) and iron (Fe) oxyhydroxide coatings that form on the limestone, because the coatings inhibit the transport, and thus neutralization, of hydrogen ions (H^+) derived from acid mine drainage.

I used mixed flow reactor experiments to investigate the effect of Al coatings on the diffusion of H^+ to the surface of limestone and to quantify how those Al coatings affect the limestone dissolution rate. Experiments used acidic Al sulfate solutions with initial Al concentrations ranging from 0.002 M to 0.01 M (32 to 329 ppm) and pH values ranging from 3.7 to 4.2, which are typical of conditions found at AMD sites. Cleaved pieces of Iceland spar calcite were used as a proxy for limestone. The pH was measured in the effluent to determine the rate of H^+ consumption. Effluent solutions were analyzed for Al, calcium (Ca) and sulfur (S) using inductively coupled plasma optical emission spectroscopy (ICP OES). Examination of the precipitated coatings using x-ray diffraction indicated that amorphous poorly crystalline gibbsite is the primary Al coating but scanning electron microscope analysis also suggests the possible presence of a poorly crystalline sulfur containing phase, such as hydrobasaluminite.

The experimental data were used to calculate the diffusion coefficient of H^+ through the Al coatings. The calculated diffusion coefficient for H^+, assuming a gibbsite and/or hydrobasaluminite layer, ranged between 10^{-13} to 10^{-11} m^2/sec, that are significantly lower than in pure water.

Effect of aluminum oxyhydroxide coatings on the performance of limestone drains

Sheyla Bethsy Palomino Ore

PUBLIC ABSTRACT

Acid mine drainage (AMD) is an acidic discharge characterized by low pH and high concentrations of toxic metals that can have an impact on the aquatic environments. A common treatment method for AMD is the use of limestone drains to neutralize the pH. However, the neutralization capacity of limestone drains can be reduced by coatings of aluminum (Al) that form on the limestone during treatment.

I used mixed flow reactor experiments to investigate the effect of Al coatings on the diffusion of H^+ to the surface of limestone and to quantify how those Al coatings affect the limestone dissolution rate. I measured pH in the effluent to determine the rate of H^+ consumption during the reaction of the solutions with calcite. I also analyzed effluent solutions for Al, Ca and S concentrations. Examination of the produced coatings with x-ray diffraction suggests amorphous poorly crystalline gibbsite as the primary Al coating but scanning electron microscope analysis also suggests the presence of poorly crystalline hydrobasaluminite, a sulfur-bearing phase.

The experimental results were used to model the decline in the limestone neutralization rate as the coatings grow thicker over time under different pH conditions and Al concentrations similar to those found in AMD. Finally, the diffusion coefficient for H^+, assuming a gibbsite and/or hydrobasaluminite layer, ranged between 10^{-13} to 10^{-11} m^2/sec, which is orders of magnitude smaller than the diffusion coefficient in pure water.

Dedication

To all who has walked by the darkness and weakness of the ignorance and didn't give up until see the brightness and success of the knowledge.

Acknowledgments

I am convinced that I was the luckiest girl in Blacksburg because I had the best mentors who helped me to design, set up and finish this thesis. First, I want to give thousands of thanks to Maddy, thanks for helping me to make all my plans work, thanks for your compression, patience and guidance, and above all thanks for being a good friend to whom I can talk freely. To Don, many thanks for all your conversations and guidance. I am very proud to have been your student. To John, many thanks for your advice, good conversations, and guidance to enter the geochemist life in Peru. To Bob, many thanks for your trust and support in the biggest adventure of my life studying in the USA.

Many thanks to all of the graduate students who shared with me short conversations about the graduate life. Listening your fears and goals made me feel stronger and not to feel alone in this experience.

Thanks to Fulbright program for giving me the opportunity to study in the USA. I will take this valuable knowledge with me to my home country, Peru.

Many thanks to my family and friends who did not doubt my capacity to finish my master's degree and who are waiting for my return home.

Table of contents

List of figures

Chapter 1. Introduction

Acid mine drainage (AMD) affects the quantity, quality and potential uses of water supplies in coal and metal mining regions worldwide (Marcus, 1997). Elevated aluminum (Al) concentrations occur in both metal mines (Plumlee et al., 1999) and coal mines (Cravotta, 2008) (Figure 1) because it is primarily leached by low pH solutions from aluminosilicate minerals in the host rocks. Although the occurrence of iron (Fe) in AMD has been widely studied, there is much less published information on the behavior of Al and Al minerals in AMD systems (Sergio Carrero, 2017).

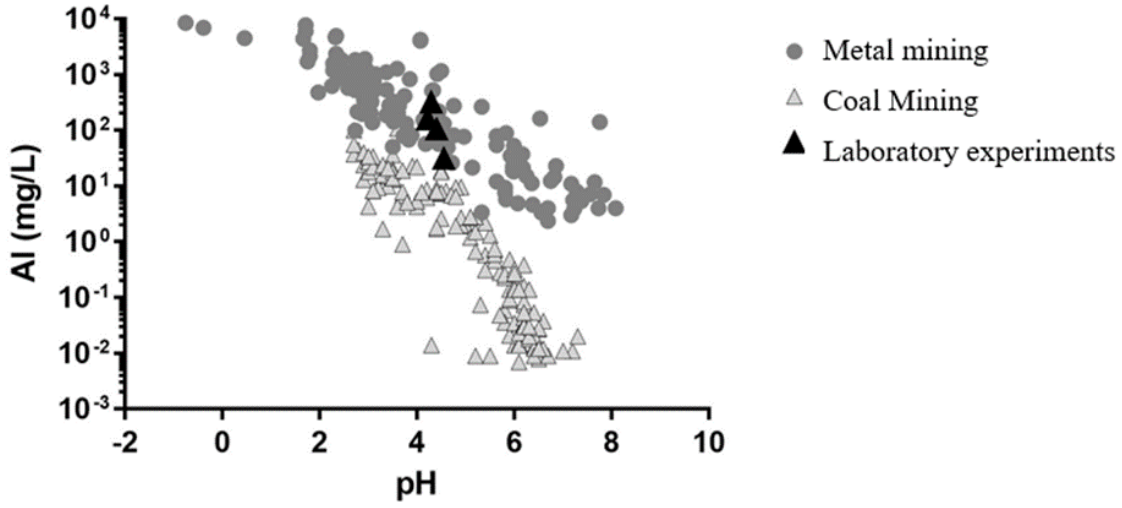

Figure 1. Dissolved Al concentrations versus pH in acid mine drainage from coal mines (Cravotta, 2008), metal mines (Plumlee et al., 1999) and for the initial conditions of the laboratory experiments described in this study.

At the low pH values of AMD, Al is easily mobilized from aluminosilicate minerals such as feldspars, micas, and clays. Water with low pH and elevated concentrations of Al can have adverse impacts on aquatic health. Aluminum toxicity to algae and fish is influenced by pH, concentrations of calcium, dissolved organic matter, fluoride and phosphorus (Gensemer and Playle, 1999). Although researchers are still working on evaluating the detailed mechanism(s) of Al toxicity, studies have shown that low pH waters with elevated Al have an adverse impact on aquatic organisms (Camargo et al., 2009; Cravotta, 2008; Gensemer and Playle, 1999; Soucek et al., 2003).

Passive treatment systems which add alkalinity are commonly used to treat AMD. The goal of these systems is to remove net acidity and metals while increasing pH and alkalinity (Cravotta, 2003; Hedin et al., 1994; Skousen et al., 2017). Anoxic limestone drains, oxic limestone drains, reducing and alkalinity producing systems, and successive alkalinity producing systems are the most frequently used passive systems for AMD treatment (Watzlaf et al., 2000). Each of these systems involves limestone, which is placed on the surface or buried in trenches or beds, sometimes with the addition of other materials such as an organic substrate (i.e., straw, mulch, manure), into which AMD is introduced. In the drain, limestone (calcite) consumes acidity by reacting with hydrogen ions from the solution to produce calcium ions and carbonic acid:

$$CaCO_3 + 2H^+ = Ca^{2+} + H_2CO_3 \quad (1)$$

One of the main problems of using limestone drains is the generation of mineral coatings on the surface of the limestone, which reduces the neutralization rate and consequently the efficiency in AMD treatment. Several studies conducted to evaluate the efficiency of the limestone drains with high concentrations of Fe, Al and dissolved sulfate have shown the rapid formation of gypsum coatings (Huminicki and Rimstidt, 2008) and Fe-Al hydroxysulfate (Hammarstrom et al., 2003; Soucek et al., 2003; Watzlaf et al., 2000).

The net acidity in AMD is the sum of the concentration of hydrogen ions and "latent acidity" which is due to hydrogen ions that can be produced mainly by the hydrolysis of Fe(II), Fe(III), Mn(II) and Al(III) (Kirby and Cravotta, 2005) (see Table 1). For example, basaluminite precipitation produces 2.5 H^+ for every Al^{3+} that is removed from the solution, and gibbsite precipitation generates 3 H^+ for every Al^{3+} that is removed from the solution. Effective limestone drains remove both free hydrogen ions and also hydrogen ions released by the hydrolysis of dissolved metals.

Nordstrom (1982) described solid-phase solubility controls on Al concentration in waters of high sulfate concentration and low pH. Al hydrolyzes in solution (see Table 1) with the continued removal of H^+ by neutralization reactions, which results in the precipitation of poorly crystalline gibbsite and basaluminite. Figure 2 is an activity diagram that shows the relationship between the different phases of Al (gibbsite, basaluminite) with different activities of H^+, Al^{3+}, and SO_4^{-2} in solution. To support these predicted relationships, there is also evidence for the presence of hydrobasaluminite in streams impacted by AMD (Sánchez-España et al., 2011; Sergio Carrero, 2017). Gibbsite has also been found as a precipitate in AMD (Sánchez-España et al., 2011) and in laboratory experiments (Farkas and Pertlik, 1997).

Table 1. Equilibrium constants for reactions involving Al^{3+}, H^+ and SO_4^{2-}

Reaction	log K	Reference
$Al(OH)_3(gib) + 3\ H^+ = Al^{3+} + 3\ H_2O$	7.74	(Palmer and Wesolowski, 1992)
$Al(OH)_3(amo) + 3\ H^+ = Al^{3+} + 3\ H_2O$	10.8	(Appelo and Postma, 2009)
$Al_4(SO_4)(OH)_{10}•5H_2O(bas) + 10\ H^+ = 4\ Al^{3+} + SO_4^{2-} + 5\ H_2O$	22.7	(Singh and Brydon, 1969)
$Al^{3+} + H_2O = AlOH^{2+} + H^+$	-5.00	(Nordstrom and May, 1996)
$Al^{3+} + 2\ H_2O = Al(OH)_2^+ + 2\ H^+$	-10.1	(Nordstrom and May, 1996)
$Al^{3+} + 3\ H_2O = Al(OH)_3^0 + 3\ H^+$	-16.8	(Nordstrom and May, 1996)
$Al^{3+} + 4\ H_2O = Al(OH)_4^- + 4\ H^+$	-22.99	(Nordstrom and May, 1996)

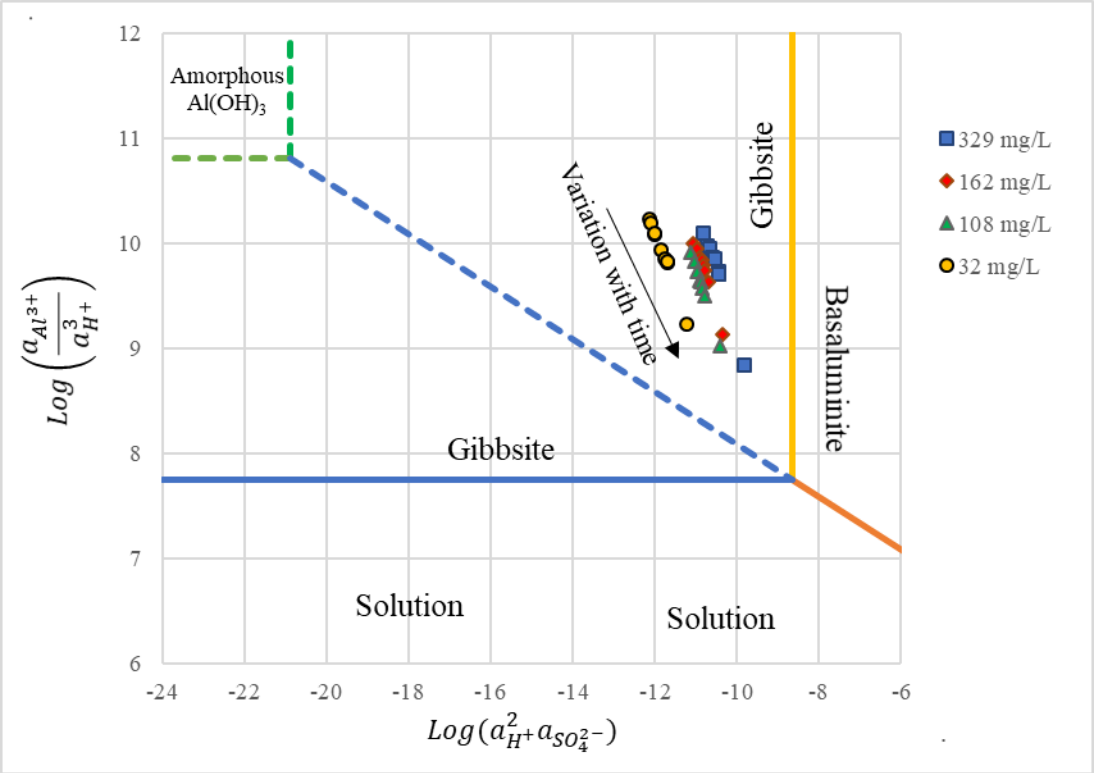

Figure 2. Activity diagram showing the relationships among the Al phases, using Al^{3+}, H^+, and SO_4^{-2} relationship in the experimental solutions. Activities were calculated with the Debye Hückel method. The colored symbols show the solution concentrations of Al^{3+} in our laboratory experiments (data included in Appendix A). Thermodynamic data used in this plot were obtained from Table 1.

Because limestone drains are relatively easy to construct, involve inexpensive and environmentally benign materials, and operate for extensive periods of time without interventions, they are widely used for passive treatment of AMD. Current designs are primarily based on knowledge acquired by empirical trial and error. Limestone drain design will incrementally improve as field experiences continue to accumulate. However, this approach tends to discourage testing of possible major enhancements because of the time required to install and monitor a constructed treatment system and the added complexity of data interpretation in a dynamic field environment. Another approach to advance ideas for improving limestone drain performance is to conduct laboratory experiments to investigate underlying chemical and physical processes. This thesis describes laboratory experiments used to examine

the interactions between a simplified AMD solution and calcite. One set of experiments is illustrated by investigating the formation of Al coatings on the calcite surfaces.

When Al precipitates in limestone drains it coats the limestone and acts as a barrier to H^+ transport to the limestone surface. As the coatings thicken, the limestone treatment becomes less efficient. The objective of this thesis is to present results from a series of mixed-flow reactor experiments along with a quantitative model to predict the declining neutralization rate caused by the formation of Al coatings. In the experiments, Al^{3+} and SO_4^{2-} concentrations were chosen such that they are in the range of values observed in field settings and undersaturated with respect to gypsum (see Figure 1). Experimental data were used to calculate the effective diffusion coefficients of H^+ through the precipitated Al coatings, to predict the thickness of the coatings, and to determine how the coatings affect the neutralization rate.

Chapter 2. Methods and Materials

Mixed flow reactor (MFR) experiments were used to study the reaction rates of different concentrations of aluminum sulfate solutions with calcite. MFRs allow for a well-mixed solution, so the discharge solution (effluent) is a representative sample of the reactor contents. As a result, the effluent concentrations reflect the solution composition that produced the observed rate (Rimstidt and Dove, 1986).

The experimental set up is shown in Figure 3. The influent solution (feed) was stored in a plastic tank with a capacity of 2000 mL. The solution was introduced into the MFR using a peristaltic pump. The MFR was manufactured by 3D printing. The design was slightly modified from the design of Michel et al. (2018) to have a space to hold crushed calcite on mesh positioned just above the stir bar. The MFR was placed on a stir plate to keep the solution well-mixed. The effluent solution was collected in 15 mL glass tubes using a fraction collector.

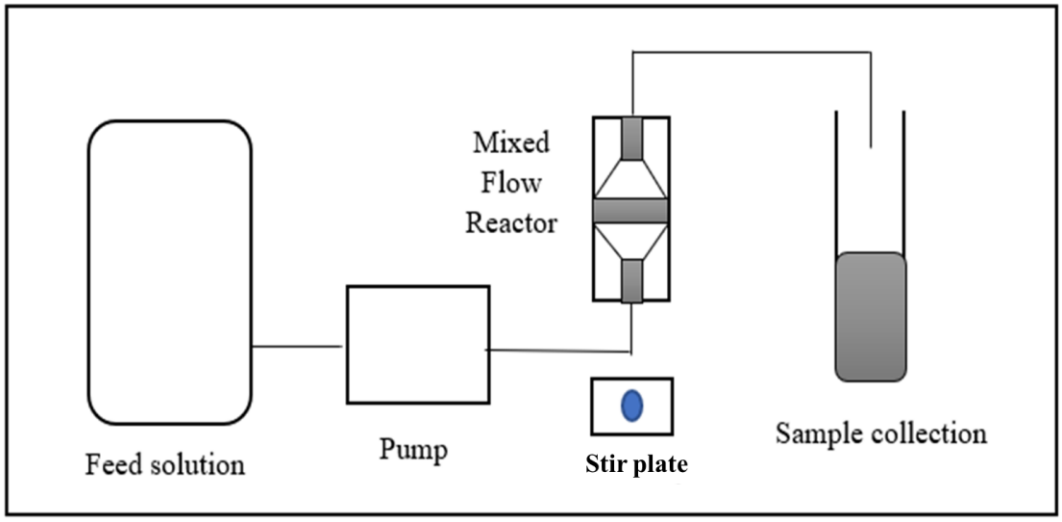

Figure 3. Schematic diagram of mixed flow reactor experiment.

Iceland spar calcite crystals used were free of visible inclusions and were crushed and sieved (18 to 20 mesh) to recover the 80 to 125 µm fractions. The specific geometric surface area was calculated to be 0.00214 m^2/g based on an average grain diameter of 100 µm. The feed solution was made by dissolving 66.601g of reagent grade $Al_2(SO_4)_3 \cdot 18H_2O$ in 1 kg deionized water to create a 0.1 *m* stock solution. This solution was diluted to yield run solutions with Al concentrations of 0.01, 0.006, 0.004, and 0.001 *m* (329, 162, 108 and 32 mg/L, respectively).

Concentrations of Al that are found in natural AMD that are undersaturated with respect to gypsum. The initial pH of the run solutions ranged between 3.76 and 4.16 due to the hydrolysis of the dissolved Al.

Experiments were performed at room temperature of 25 ± 1°C. At the beginning of each experiment 2.1 g of the crushed calcite was placed on the mesh and feed solution was then pumped into the reactor at a rate of approximately 0.02 g/sec. The experiment began (time = 0) when the solution first discharged from the reactor.

Effluent solution was collected into pre-weighed 15 mL tubes every 9 minutes. The sample tubes were weighed before and after sample collection, and the amount of solution collected was divided by the collection time to calculate the flow rate. The pH was measured using an Ag/AgCl pH electrode calibrated with buffers at pH values of 7.00 and 4.00 for each measurement. The samples were acidified with nitric acid (to pH < 2) to preserve for chemical analysis. Each experiment ran for between 3 and 4 hours.

After each experiment, the calcite grains were recovered, dried and stored in plastic tubes. Fluxes of species (J_i) between the solution and calcite surfaces (mol/m^{2}sec) were calculated from the difference between feed and effluent solution concentrations (mol/kg), multiplied by the flow rate (kg/sec), and divided by the total surface area of the calcite (m^2) (Rimstidt and Newcomb, 1993).

To obtain sufficient Al coating in the batch reactor for X-ray diffraction (XRD) and scanning electron microscopy (SEM) analysis, pieces (0.5 x 0.5 x 0.1 cm) of Iceland spar calcite with cleavage surfaces were immersed in three different concentrations of aluminum sulfate solution (0.01, 0.004 and 0.002 M Al (270, 108 and 54 mg/L, respectively) for 168 hours (7 days)). After the formation of a sufficient quantity of coating to analyze, the calcite pieces were recovered and dried for analysis. Coating were also analyzed in the MFR experiments.

The total Al, Ca, and S concentrations in the feed and sample solutions were measured using inductively coupled plasma - optical emission spectroscopy (Spectro Arcos ICP-OES) at the Virginia Tech Soil and Plant Analysis Laboratory. The samples were not filtered and there was no evidence of precipitates in solution before adding nitric acid. Sulfate was calculated from

the S concentrations assuming that sulfate was the only S species in solution. The Al coating represents the difference between the Al concentration in the influent and the effluent from the reactor. Repeat measurements of selected samples showed agreement between the samples of ± 2.75 % (n=2). XRD patterns of the Al coating were obtained using a benchtop X-ray diffractometer (Rigaku) with a diffracted beam monochromator for Cu radiation (Cu Kα) with a scan range of 3 to 88° 2ɵ, and a scan rate of 0.02° 2ɵ/min and an accuracy better than 0.01°. A Hitachi Tabletop Scanning Electron Microscope (SEM) TM3000 instrument with energy dispersive spectral analysis (EDS) was used to image the coatings on the reacted grains and to conduct qualitative chemical mapping.

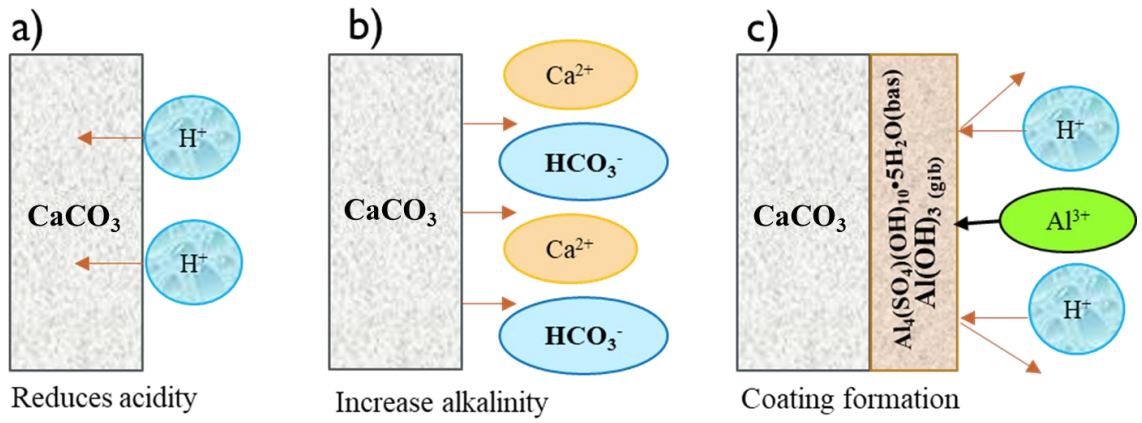

Figure 4. Limestone theoretical interaction with aluminum sulfate a) reduce acidity b) increase alkalinity and c) Al coating formation.

Chapter 3. Results

The Al concentrations in the effluent (Figure 5) were always lower than the influent Al concentrations due to the precipitation of the Al as a coating on the calcite surface. As the experiment progressed, the effluent Al concentration steadily increased and reached an approximate steady state within 2 to 3 hours. By the end of the experiment, the final effluent Al concentrations were between 80 and 93% of the influent concentration (93, 92, 91 and 80% for the initial Al concentrations of 329, 162, 108 and 32 mg/L, respectively). As the Al coating formed on calcite, the effluent solution hydrogen ion concentration increased (pH values decreased) as shown in Table 2 and Figure 5, which indicates that the rate of H^+ consumption by the neutralization process decreased over the course of the experiment (Appendix B). Calcium concentrations were higher at the beginning of the experiment and decreased with time, as the rate of Ca^{2+} production by calcite dissolution decreased (see equation 1) which is the opposite trend compared to aluminum concentrations (Figure 5). In contrast, sulfate concentrations in solution did not change significantly with time (Figure 5). This suggests that sulfate was not removed from solution in significant quantities (i.e., gypsum or basaluminite precipitation, Appendix C).

Table 2. Hydrogen ion concentration variations between effluent and influent in the experiments.

Initial Al (mg/L)	H^+ influent	H^+ effluent (mg/L)		H^+ variation (mg/L)	
		start	end	start	end
329	1.74E-04	5.50E-05	8.71E-05	3.16E-01	5.01E-01
162	1.17E-04	5.13E-05	7.76E-05	4.37E-01	6.61E-01
108	1.17E-04	5.37E-05	7.94E-05	4.57E-01	6.76E-01
32	7.24E-05	2.57E-05	4.27E-05	3.55E-01	5.89E-01

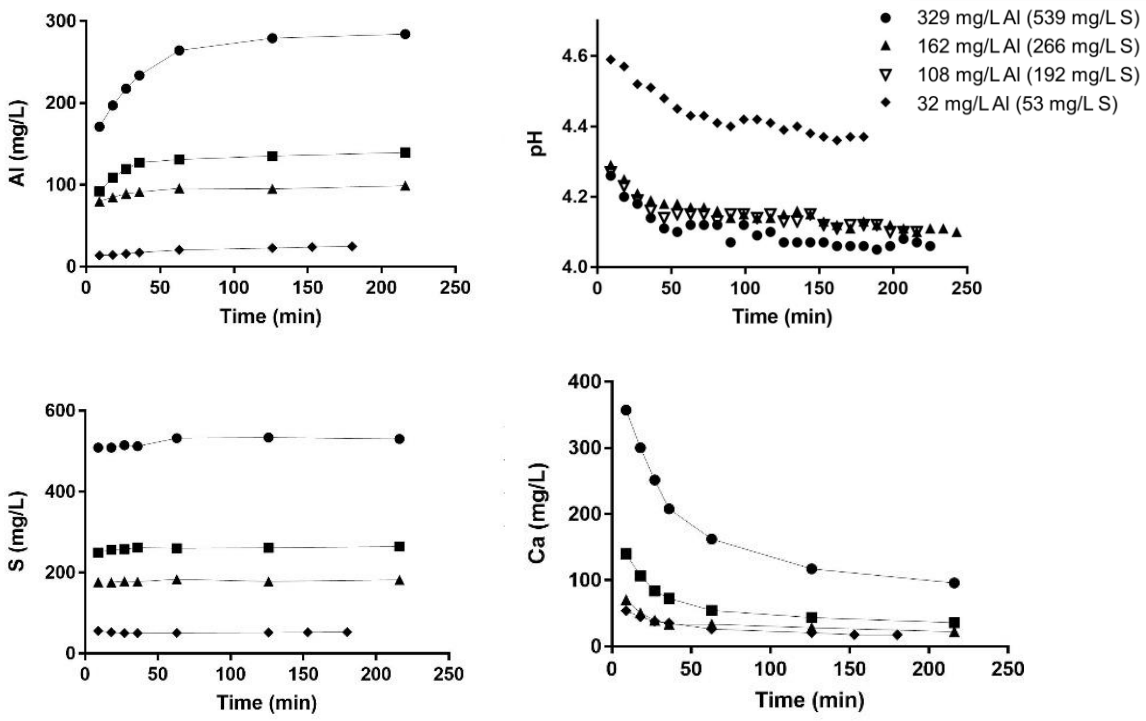

Figure 5. Measured pH and concentrations of Al, Ca, and S in the effluent solutions over time for different initial Al concentrations in the MFR experiments.

The MFR experiments were repeated at least twice for each concentration of aluminum sulfate to ensure their replicability. The pH measurements for the duplicate 329, 169, 108 and 32 mg/L Al experiments showed a difference of ±0.49, 3.31, 6.32 and 2.46 % respectively (Appendix D: table and graph). Replicate measurements of Al, Ca and S for selected samples in the experiments were within ± 5.1% of each other (Appendix E).

The SEM was used to analyze coatings on the calcite surface produced from the MFR experiments. A back-scattered electron image of one coating and chemical maps (Al, and S) of the coating are shown in Figure 6 for the 32 mg/L Al experiment after 4 hours. These maps indicate some S is present in the coating (Figure 6c), suggesting that minor amounts of basaluminite may have formed in the experiment, although the mass percent of sulfur is quite low (<3%) in coating (Figure 6d). Additional SEM for batch reactor can be seen in Appendix F.

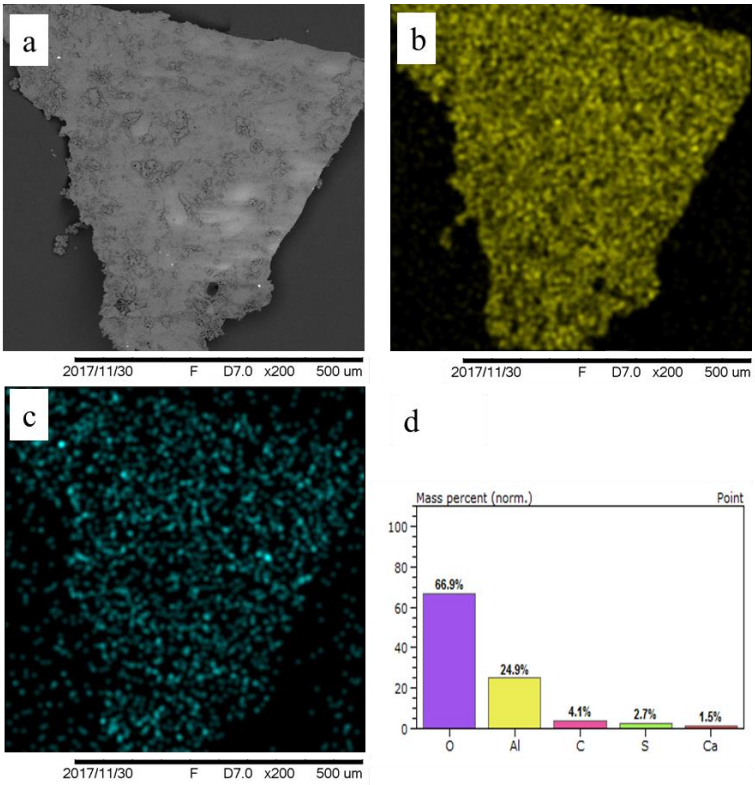

Figure 6. a) SEM back-scattered image of coating for the 32 mg/L Al formed after 4 hours in a MFR experiments. Concentrations maps of b) Al and c) S and d) Semi – qualitative molar ratio of 11:1 Al:S. Maps are of the same field of view. Brighter colors in the Al and S maps reflect higher concentrations.

In the batch experiments, a white film appeared on the surface of calcite after 1 hour. After 3 hours, a distinct coating had formed on the calcite surface (Figure 7). This coating was collected for XRD analysis. XRD analysis of the coating material formed with an initial aluminum concentration of 270 mg/l indicates that the coating consists primarily of poorly crystalline gibbsite (Figure 8) based on matching the peaks to the diffraction pattern. Additional XRD patterns can be seen in Appendix G at Al concentrations of 54 mg/l and 108 mg/l and also support the interpretation of the poorly crystalline peaks corresponding primarily to gibbsite.

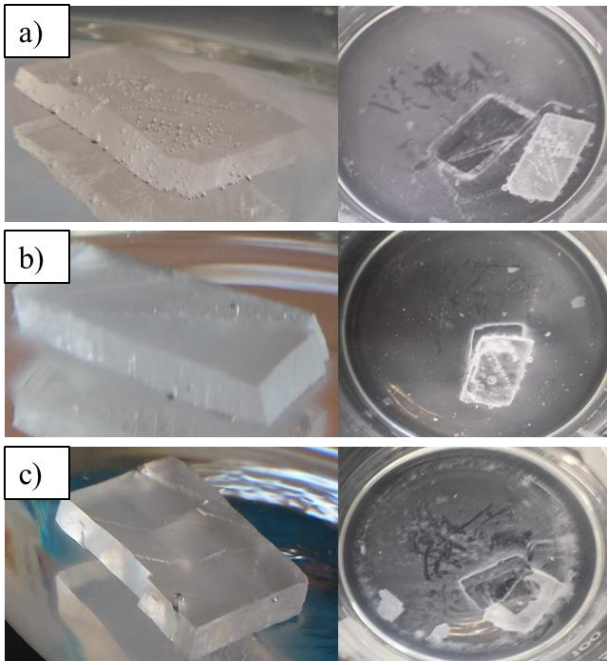

Figure 7. Pictures of the precipitate on the calcite from the batch experiments with Al concentrations of a) 270 mg/L b) 108 mg/L c) 54 mg/L (diameter of petri dish is 9 cm) that formed after 4 hours.

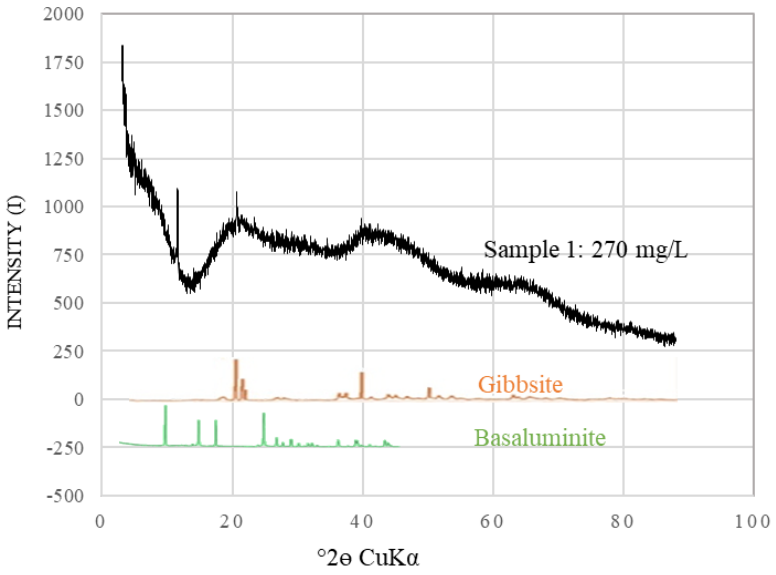

Figure 8. XRD pattern for the 270 mg/L Al experiment indicating that the coating material is predominantly poorly crystalline gibbsite. The patterns for well crystallized gibbsite (orange) and basaluminite (green) are shown for comparison.

Chapter 4. Discussion

Results of the experiments were used to calculate the diffusion coefficient for H^+ transport through the Al coatings. The assumption of the diffusion model is that the coating acts as a barrier, hindering the diffusive transport of H^+ between the solution and the calcite surface. To calculate the diffusion coefficient, we first examine the stoichiometry of the reactions producing either gibbsite or basaluminite (the predicted coatings, see Figure 2) to calculate the flux model of hydrogen in the system. The variables of our model are time, and the concentration of H^+, Al^{3+}, Ca and SO_4^{2-}.

The reaction of aluminum ± sulfate with calcite increases the solution pH, causing Al hydroxide (gibbsite) and/or Al hydroxysulfate (basaluminite) phases to precipitate (see Figure 2). Aluminum precipitation produces hydrogen ions. Gibbsite precipitation generates 3 H^+ for every Al^{3+} that is removed from the solution:

$$Al^{3+} + 3\ H_2O = Al(OH)_3(gib) + 3\ H^+ \qquad (2)$$

Basaluminite precipitation produces 2.5 H^+ for every Al^{3+} that is removed from the solution:

$$4\ Al^{3+} + SO_4^{2-} + 15\ H_2O = Al_4(SO_4)(OH)_{10}\bullet 5H_2O(bas) + 10\ H^+ \qquad (3)$$

The relative rates of these reactions can be determined by comparing the fluxes of the various reacting species into or out of the solution. Here we define fluxes of dissolved species from the solution to the solids as negative values ($-J_i$) and from the solids to the solution as positive values ($+J_i$). These fluxes are calculated from the difference between their concentration in the feed ($m_{i,f}$) and discharge ($m_{i,d}$) solutions, the solution flow rate (r_f), and the calcite surface area (A):

$$J_i = \frac{\left(m_{i,f} - m_{i,d}\right) r_f}{A} \qquad (4)$$

The fluxes for H^+, Al^{3+}, Ca^{2+} and SO_4^{2-} calculated for the 329 mg/L experiment are shown in Table 3 (calculations for all experiments are in Appendix H) and shown in Figure 9.

Table 3. Fluxes (mol/m^2.sec) calculated for the 329 mg/L experiment

t sec	J(Al) mol/m^{2}sec	J(Ca) mol/m^{2}sec	J(S) mol/m^{2}sec	J(H) mol/m^{2}sec	J(cal) mol/m^{2}sec	J(bas) mol/m^{2}sec	J(gib) mol/m^{2}sec	J(Al$_{out}$) mol/m^{2}sec
540	-2.32E-05	4.16E-05	-4.44E-06	-5.55E-07	-8.32E-05	4.44E-05	1.63E-05	2.31E-05
1080	-1.84E-05	3.44E-05	-4.33E-06	-5.09E-07	-6.88E-05	4.33E-05	3.31E-06	2.28E-05
1620	-1.48E-05	2.86E-05	-3.48E-06	-4.91E-07	-5.72E-05	3.48E-05	2.62E-06	2.03E-05
2160	-1.21E-05	2.37E-05	-3.83E-06	-4.64E-07	-4.74E-05	3.83E-05	-9.77E-06	1.93E-05
3780	-6.99E-06	1.87E-05	-9.62E-07	-4.54E-07	-3.75E-05	9.62E-06	9.42E-06	1.89E-05
7560	-4.06E-06	1.25E-05	-7.34E-07	-3.78E-07	-2.49E-05	7.34E-06	3.37E-06	1.46E-05
12960	-3.53E-06	1.10E-05	-1.27E-06	-3.97E-07	-2.19E-05	1.27E-05	-4.61E-06	1.42E-05

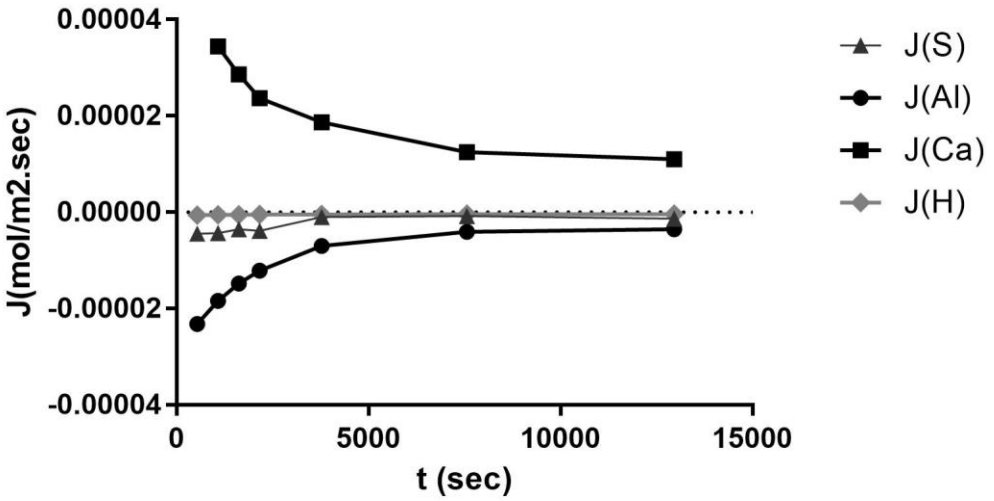

Figure 9. Calculated sulfur, aluminum, calcium and hydrogen fluxes (mol/m^{2}sec) in the 329 mg/L Al experiment over time.

Although these calculated fluxes contain potential information about the reactions that are occurring in the reactor, there are some problems. Because the S flux is calculated from minor differences in relatively large numbers, the S flux values have large associated errors. Those errors propagate to decrease the accuracy of the basaluminite and gibbsite precipitation flux calculation, and they are likely responsible for the occurrence of negative J_{gib} values in Table 3.

However, these calculations support the possibility that some basaluminite formed in the coatings near the calcite surface where the pH was higher than the surrounding solution where gibbsite is the stable phase.

The coating thickness (x, m) was calculated as the number of moles of Al deposited per square meter (n_{Al}, mol/m^2) multiplied by the molar volume of the coating (V_m, m^3/mol) and divided by ($1-\phi$) where ϕ is the porosity:

$$x = \frac{n_{Al} V_m}{1 - f} \qquad (5)$$

In our calculations ϕ was set at 0.5. Unit cell volume data (from http://webmineral.com/) were used to calculate the molar volumes. The basaluminite unit cell contains 24 formula units and has a volume of 8385.70 Å^3. This translates to a molar volume of 2.104×10^{-4} m^3. There are four moles of Al per formula unit so every mole of Al hydroxysulfate precipitated as basaluminite amounts to 5.261×10^{-5} m^3. The gibbsite unit cell contains 8 formula units and has a volume of 53.055 Å^3. This translates to a molar volume of 3.196×10^{-5} m^3. There is only one mole of Al in a mole of gibbsite.

The number of moles of Al removed from solution per square meter of calcite surface (n_{Al}) was calculated by numerical integration of J_{Al} using the trapezoidal rule and the results are shown in Table 4. The n_{Al} values were used to calculate the coating thicknesses assuming that it was either pure basaluminite or pure gibbsite. Those calculated thicknesses are on the order of a few micrometers, which is consistent with SEM observations of coatings that are slightly thinner due to dehydration. Results of the coating thickness calculations are shown in Figure 10.

Table 4. Calculated coating thickness (x, m) and H^+ diffusion coefficient in a basaluminite (D_{bas}) coating or a gibbsite (D_{gib}) coating. These calculations assume that J_{Al} from 0 to 540 sec was the same as the value calculated at 540 sec. The trapezoidal rule assumes that the flux changed as a linear function of time between sampling times.

t (sec)	J(Al) mol/m^{2}sec	J(-H) mol/m^{2}sec	n(Al) mol	x(bas) m	x(gib) m	cH*, mol/m^3	LogD$_{bas}$	LogD$_{gib}$
0	2.32E-05		0					
540	2.32E-05	1.66E-04	0.006	6.59E-07	4.01E-07	54.95	-11.70	-11.92
1080	1.84E-05	1.38E-04	0.017	1.84E-06	1.12E-06	63.10	-11.40	-11.61
1620	1.48E-05	1.14E-04	0.026	2.78E-06	1.69E-06	66.07	-11.32	-11.53
2160	1.21E-05	9.48E-05	0.034	3.55E-06	2.16E-06	72.44	-11.33	-11.55
3780	6.99E-06	7.50E-05	0.049	5.17E-06	3.15E-06	75.86	-11.29	-11.51
7560	4.06E-06	4.98E-05	0.070	7.37E-06	4.48E-06	85.11	-11.37	-11.58
12960	3.53E-06	4.38E-05	0.091	9.52E-06	5.79E-06	87.10	-11.32	-11.54

(*) cH (mol, m^3) hydrogen ion concentration in the solution.

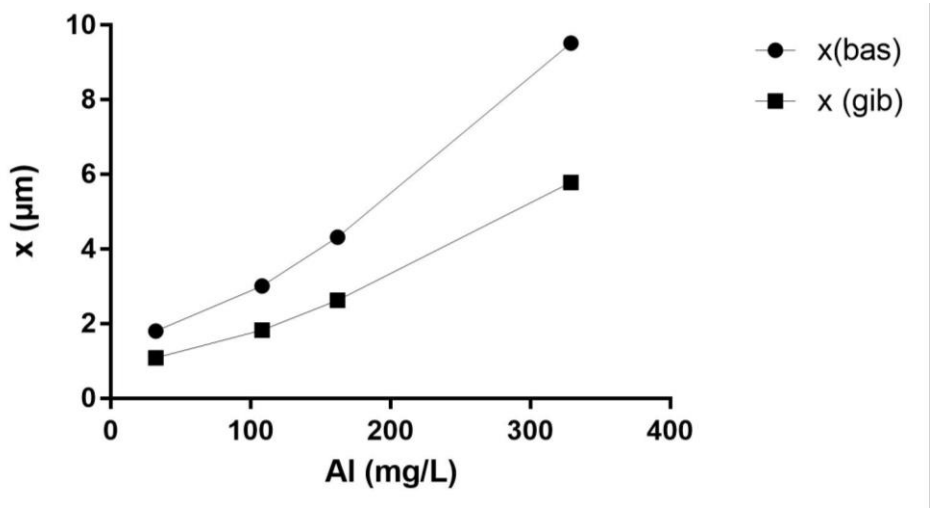

Figure 10. Calculated coating thickness produced after 216 minutes of reaction time in experiments with different Al concentrations.

Fick's first law states that the hydrogen ion diffusion flux through the coating, assuming a zero H^+ concentration at the calcite surface, is:

$$J = \frac{D}{x}\left(c_{H^+} - 0\right) \qquad (6)$$

We assumed that the hydrogen ion flux at the surface equals twice the calcium ion flux back into the solution. Equation (6) was rearranged to solve for the diffusion coefficient (D, m^2/sec).

$$D = \frac{J_H x}{c_H} \qquad (7)$$

where c_H (mol/m^3) is the hydrogen ion concentration in the solution. The calculations are shown in Appendix H. Figure 11 shows the resulting estimates of the diffusion coefficient of hydrogen ions through the coating. Note that the value chosen for the coating porosity (we used 0.5) has a minor effect on the calculated diffusion coefficient compared to the effect of the Al concentration.

Figure 11 shows that the H^+ diffusion coefficient in coatings formed from solutions with low Al^{3+} concentrations (32 and 108 mg/L) is approximately 2.51×10^{-13} m^2/sec. We interpret this result to mean that even though the coatings are relatively thin, they are very dense with a very high tortuosity. Conversely, the calculated diffusion coefficient in the coatings that formed from higher Al solutions (329 mg/L) approximately 3.09×10^{-12} m^2/sec, is ten times higher than for the lower Al solutions. These results suggest that that coating, which grew at a much faster rate in the higher Al solutions, was much less dense. The coating thickness and diffusion coefficient seems to have the effective neutralization lifetime about different the Al^{3+} concentration.

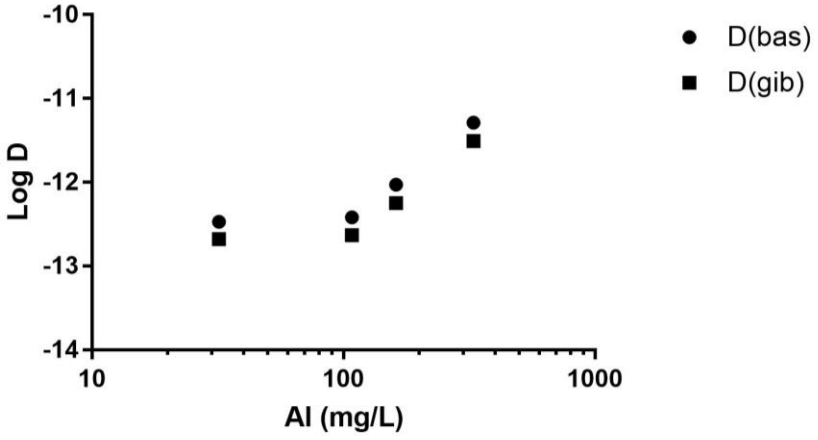

Figure 11. Calculated H^+ diffusion coefficients in the coatings that formed on the calcite in experiments with various Al concentrations. For comparison, the H^+ diffusion coefficient in pure water is $10^{-8.03}$ m^2/sec (Miller, 1982).

Over the longer term, coatings will continue to form on the calcite until the rate of H^+ neutralization becomes insignificant. At that time the effluent chemistry will nearly equal the influent chemistry.

Figure 12 shows that the hydrogen ion flux (J) from the solution to the calcite surface declines as an approximate linear function of the square root of time. That function has the form.

$$J = bt^{0.5} + J_o \qquad (8)$$

where b is the slope of the line and the intercept, J_o, is the flux at zero time, before any coating has formed. This can be rearranged to solve for $t^{0.5}$ as a function of the fractional flux remaining ($f = J/J_o$).

$$t^{0.5} = \frac{J - J_o}{b} = \frac{fJ_o - J_o}{b} = \frac{J_o(f - 1)}{b} \qquad (9)$$

Note that both (f - 1) and b are negative numbers so $t^{0.5}$ is always positive. For the 329 mg/L experiment J_o = 1.724x10^{-4} mol/m^{2}sec and b = -1.298x10^{-6} (mol/m^{2}sec)/sec$^{0.5}$. The time when the neutralization rate drops to 1 % of the original rate (f = 0.01) is

$$t^{0.5} = \frac{1.724x10^{-4}(0.01 - 1)}{-1.298x10^{-6}} = \frac{-1.707x10^{-4}}{-1.298x10^{-6}} = 131.5$$

$$t = 17290\ sec = 288\ hr = 12\ days$$

We can use results of these experiments and this model to estimate how long the calcite will effectively neutralize the hydrogen ions from AMD.

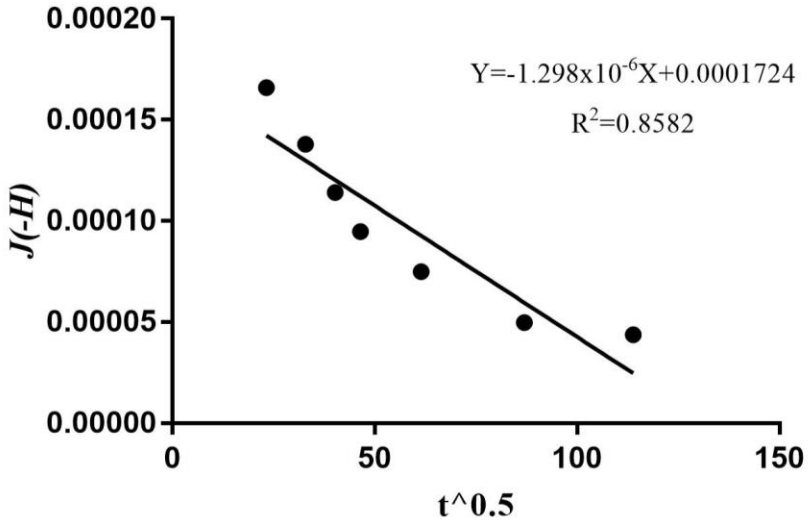

Figure 12. Diffusion flux of hydrogen ions to the calcite surface as a function of the square root of time (sec) for 329 mg/L Al.

The mixed flow reactor experiment showed that the Al oxyhydroxide coating did not adhere strongly to the surface of the calcite as it was easily removed by strong stirring and when they were dried. This suggests that Al coatings in limestone drains could possibly be removed by flushing with large amounts of water or removing the neutralization material and using different physical agitation methods to remove the coatings. This was also observed in the bath reactor.

Results of the MFR experiments indicate that the calcite neutralization rate drops quickly after exposure of the calcite to Al sulfate solution. An actual limestone drain would likely continue to function past these times. Initially, most of the Al will be removed from solution near the entrance of the drain so the downstream limestone will not be coated. The coating front would then move slowly through the length of the drain until it reaches the outlet. This arrival would mark the slowing of the neutralization ability and ultimately the failure time for the drain. Note that the slope of the J versus $t^{0.5}$ curve appears to decline with time. This decrease in rate suggests that the first-formed coatings are denser and are a more effective diffusion barrier whereas those that formed later have a lower diffusion coefficient and have less effect on hydrogen ion transport. This trend suggests that the b term in the equation may become smaller even as the coating thickness increases, which would help to extend the effective lifetime of the limestone (Santomartino and Webb, 2007). In actual limestone drains, the coating will consist of

a mixture of Al and iron oxyhydroxides. The iron oxyhydroxides may disrupt the structure of the Al oxyhydroxide deposits and thus increase the overall diffusion coefficient of the mixed coating. There is also the possibility of the gypsum precipitation from these high sulfate solutions which could impact the Al coatings and possibly allow faster diffusion of the hydrogen ion. Finally, if the later-formed coatings are less dense, in real limestone channels they may be removed by flushing during rain events, which would reset the coatings to smaller thicknesses and revive the neutralization effectiveness.

Chapter 5. Conclusion

Improvement of the performance of limestone drains requires knowledge gained from four sources. First, laboratory experiments, like the one described here, are needed to understand the underlying chemistry and physics of the flow and neutralization processes. Second, pilot scale tests (Cravotta III, 2003; Cravotta III et al., 2004) are needed to determine how well models developed from laboratory studies can be scaled to field conditions. Third, monitoring of the behavior of installed drains (Hedin et al., 1994; Skousen and Ziemkiewicz, 2005; Watzlaf et al., 2000) is needed to determine whether their performance matches the predictions of the design models. Finally, post mortem failure analyses of defunct limestone drains are needed to establish the reasons for declining performance (Hammarstrom et al., 2003).

The experiment described here provides a rapid and inexpensive way to test the effect of a wide range of solution chemistry on limestone neutralization rates. It can also be used to test the neutralization behavior of related solids such as dolomite (Genty et al., 2012), magnesite (Masindi et al., 2015), and steel slag (Simmons et al., 2001). The experiment shows how changing pH and the solution concentration of coating-forming species affect coating growth rates and properties. It can also test the effects of possible coating modifiers, such as surfactants, on neutralization rates. Collecting and analyzing this kind of information are a first step toward improving the models used for limestone drain designs.

References

Appelo, C.A.J. and Postma, D. (2009) Geochemistry, groundwater and pollution, 2nd ed. CRC Press, Boca Raton, Fl.

Camargo, M.M.P., Fernandes, M.N. and Martinez, C.B.R. (2009) How aluminium exposure promotes osmoregulatory disturbances in the neotropical freshwater fish Prochilus lineatus. Aquatic Toxicology 94, 40-46.

Cravotta, C.A. (2003) Size and performance of anoxic limestone drains to neutralize acidic mine drainage. Journal of Environmental Quality 32, 1277-1289.

Cravotta, C.A. (2008) Dissolved metals and associated constituents in abandoned coal-mine discharges, Pennsylvania, USA. Part 1: Constituent quantities and correlations. Applied Geochemistry 23, 166-202.

Cravotta III, C.A. (2003) Size and performance of anoxic limestone drains to neutralize acid mine drainage. Journal of Environmental Quality 32, 1277-1289.

Cravotta III, C.A., Ward, S.J., Koury, D.J. and Koch, R.D. (2004) Optimization of limestone drains for long-term treatment of mine drainage, Swarara Creek basin, Schulykill County, PA, 2004 National Meeting of the American Society of Mining and Reclamation. ASMR, Lexington, KY, pp. 366-411.

Gensemer, R.W. and Playle, R.C. (1999) The Bioavailability and Toxicity of Aluminum in Aquatic Environments. Critical Reviews in Environmental Science and Technology 29, 315-450.

Genty, T., Bussirére, B., Potvin, R., Benzaazoua, M. and Zagury, G.J. (2012) Dissolution of calcitic marble and dolomitic rock in high iron concentrated acid mine drainage: application to anoxic limestone drains. Environmental Earth Science 66, 2387-2401.

Hammarstrom, J.M., Sibrell, P.L. and Belkin, H.E. (2003) Characterization of limestone reacted with acid-mine drainage in a pulsed limestone bed treatment system at the Friendship Hill National Historical Site, Pennsylvania, USA. Applied Geochemistry 18, 1705-1721.

Hedin, R.S., Watzlaf, G.R. and Nairn, R.W. (1994) Passive Treatment of Acid Mine Drainage with Limestone. Journal of Environmental Quality 23, 1338-1345.

Huminicki, D.M.C. and Rimstidt, J.D. (2008) Neutralization of sulfuric acid solutions by calcite dissolution and the application to anoxic limestone drain design. Applied Geochemistry 23, 148-165.

Kirby, C.S. and Cravotta, C.A. (2005) Net alkalinity and net acidity 2: Practical considerations. Applied Geochemistry 20, 1941-1964.

Marcus, J.J. (1997) Mining Environmental Handbook. Imperial College Press, London.

Masindi, V., Gitari, M.W., Tutu, H. and DeBeer, M. (2015) Passive remediation of acid mine drainage using cryptocrystalline magnesite: A batch experimental and geochemical modelling approach. Water SA 41, 677-682.

Michel, F.M., Rimstidt, J.D. and Kletetschka, K. (2018) 3D printed mixed flow reactor for geochemical rate measurements. Applied Geochemistry 89, 86-91.

Miller, D. (1982) Estimation of tracer diffusion coefficients of ions in aqueous solution. Lawrence Livermore National Lab., CA (USA).

Nordstrom, D.K. (1982) The effect of sulfate on aluminum concentrations in natural waters: some stability relations in the system Al2O3-SO3-H2O at 298 K. Geochimica et Cosmochimica Acta 46, 681-692.

Palmer, D.A. and Wesolowski, D.J. (1992) Aluminum speciation and equilibria in aqueous - solution. 2. The solubility of gibbsite in acidic sodium - chloride solutions from 30-degrees-C to 70-degrees-C. Geochimica et cosmochimica acta 56, 1093-1111.

Plumlee, G.S., Smith, K., Montour, M., Ficklin, W. and Mosier, E. (1999) Geologic controls on the composition of natural waters and mine waters draining diverse mineral-deposit types.

Rimstidt, J.D. and Dove, P.M. (1986) Mineral/solution reaction rates in a mixed flow reactor: Wollastonite hydrolysis. Geochimica et Cosmochimica Acta 50, 2509-2516.

Rimstidt, J.D. and Newcomb, W.D. (1993) Measurement and analysis of rate data: The rate of reaction of ferric iron with pyrite. Geochimica et Cosmochimica Acta 57, 1919-1934.
Sánchez-España, J., Yusta, I. and Diez-Ercilla, M. (2011) Schwertmannite and hydrobasaluminite: A re-evaluation of their solubility and control on the iron and aluminium concentration in acidic pit lakes. Applied Geochemistry 26, 1752-1774.
Santomartino, S. and Webb, J.A. (2007) Estimating the longevity of limestone drains in treating acid mine drainage containing high concentrations of iron. Applied Geochemistry 22, 2344-2361.
Sergio Carrero, A.F.-M., Rafael Pérez-López, Daniel Lee, Giuliana Aquilanti, Agnieszka Poulain, Alba Lozano, José-Miguel Nieto (2017) The nanocrystalline structure of basaluminite, an aluminum hydroxide sulfate from acid mine drainage. American Mineralogist 102, 2381-2389.
Simmons, J., Ziemkiewicz, P. and Black, D.C. (2001) Use of steel slag leach beds for the treatment of acid mine drainage, 2001 National Association of Abandoned Mine Lands Annual Conference, Athens, Ohio.
Singh, S.S. and Brydon, J.E. (1969) Solubility of basic aluminum sulfates at equilibrium in solution and in the presence of montmorillonite. Soil Science 107, 12-16.
Skousen, J. and Ziemkiewicz, P. (2005) Performance of 116 passive treatment systems for acid mine drainage, 2005 National Meeting for the American Society of Mining and Reclamation. ASMR, Breckenridge, CO.
Skousen, J., Zipper, C.E., Rose, A., Ziemkiewicz, P.F., Nairn, R., McDonald, L.M. and Kleinmann, R.L. (2017) Review of Passive Systems for Acid Mine Drainage Treatment. Mine Water and the Environment 36, 133-153.
Soucek, D.J., Cherry, D.S. and Zipper, C.E. (2003) Impacts of Mine Drainage and Other Nonpoint Source Pollutants on Aquatic Biota in the Upper Powell River System, Virginia. Human and Ecological Risk Assessment: An International Journal 9, 1059-1073.
Watzlaf, G.R., Schroeder, K.T. and Kairies, C.L. (2000) Long-term performance of anoxic limestone drains. Mine Water and the Environment 19, 98-110.

Appendix A: Debye Hüeckel calculations of activities of Al^{3+}, Ca^{2+}, SO_4^{-2} and H^+ for the graph of Al phases

Solution Al mg/L	Time (sec)	Al^{3+} mol/L	Ca^{2+} mol/L	SO_4^{-2} mol/L	H^+ mol/L	I	Al^{3+} mol/L	Ca^{2+} mol/L	SO_4^{-2} mol/L	H^+ mol/L	Activity Al^{3+}	Activity Ca^{2+}	Activity SO_4^{-2}	Activity H^+	$\log((H^+)^2.SO_4^{-2})$	$\text{Log}(Al^{3+}/(H^+)^3)$
		z=3	z=2	z=-2	z=1	0.5*z^2*C	z=3 n=0.9	z=2 n=0.6	z=-2 n=0.4	z=1 n=0.9						
329-1	Feed	0.0113	0.0000	0.0168	0.0002	0.085	0.192	0.421	0.373	0.833	2.17E-03	9.13E-07	6.28E-03	1.45E-04	-9.88	8.86
	9	0.0063	0.0089	0.0159	0.0001	0.078	0.199	0.430	0.384	0.836	1.26E-03	3.83E-03	6.10E-03	4.59E-05	-10.89	10.11
	18	0.0073	0.0075	0.0159	0.0001	0.080	0.197	0.428	0.381	0.835	1.44E-03	3.20E-03	6.06E-03	5.27E-05	-10.77	9.99
	27	0.0081	0.0063	0.0161	0.0001	0.081	0.196	0.426	0.379	0.834	1.58E-03	2.67E-03	6.09E-03	5.51E-05	-10.73	9.97
	36	0.0087	0.0052	0.0160	0.0001	0.081	0.196	0.425	0.378	0.834	1.69E-03	2.20E-03	6.05E-03	6.04E-05	-10.66	9.88
	63	0.0098	0.0040	0.0166	0.0001	0.085	0.191	0.419	0.372	0.832	1.87E-03	1.70E-03	6.19E-03	6.31E-05	-10.61	9.87
	126	0.0103	0.0029	0.0167	0.0001	0.086	0.191	0.419	0.371	0.832	1.98E-03	1.22E-03	6.19E-03	7.08E-05	-10.51	9.75
	216	0.0105	0.0024	0.0166	0.0001	0.085	0.192	0.420	0.372	0.832	2.02E-03	1.00E-03	6.16E-03	7.25E-05	-10.49	9.72
162-1	Feed	0.0056	0.0000	0.0083	0.0001	0.042	0.261	0.505	0.470	0.861	1.46E-03	8.69E-07	3.91E-03	1.01E-04	-10.40	9.15
	9	0.0034	0.0035	0.0078	0.0001	0.038	0.272	0.517	0.484	0.865	9.25E-04	1.80E-03	3.76E-03	4.44E-05	-11.13	10.02
	18	0.0040	0.0027	0.0080	0.0001	0.039	0.267	0.512	0.478	0.864	1.08E-03	1.36E-03	3.82E-03	4.86E-05	-11.04	9.97
	27	0.0044	0.0021	0.0081	0.0001	0.040	0.265	0.510	0.476	0.863	1.17E-03	1.07E-03	3.83E-03	5.32E-05	-10.97	9.89
	36	0.0047	0.0018	0.0082	0.0001	0.041	0.263	0.507	0.472	0.862	1.24E-03	9.17E-04	3.86E-03	5.57E-05	-10.92	9.86
	63	0.0049	0.0014	0.0081	0.0001	0.041	0.264	0.508	0.473	0.862	1.28E-03	6.88E-04	3.84E-03	5.83E-05	-10.88	9.81
	126	0.0050	0.0011	0.0082	0.0001	0.041	0.263	0.507	0.473	0.862	1.32E-03	5.50E-04	3.86E-03	6.10E-05	-10.84	9.76
	216	0.0052	0.0009	0.0083	0.0001	0.042	0.261	0.506	0.471	0.862	1.35E-03	4.52E-04	3.89E-03	6.69E-05	-10.76	9.66
108-1	Feed	0.0040	0.0000	0.0060	0.0001	0.030	0.299	0.546	0.516	0.874	1.19E-03	0.00E+00	3.10E-03	1.03E-04	-10.48	9.04
	9	0.0029	0.0018	0.0055	0.0001	0.028	0.308	0.555	0.527	0.877	9.07E-04	9.77E-04	2.90E-03	4.71E-05	-11.19	9.94
	18	0.0031	0.0013	0.0055	0.0001	0.028	0.309	0.556	0.528	0.878	9.67E-04	7.03E-04	2.89E-03	5.17E-05	-11.11	9.85
	27	0.0033	0.0010	0.0056	0.0001	0.028	0.307	0.555	0.526	0.877	1.01E-03	5.48E-04	2.93E-03	5.66E-05	-11.03	9.75
	36	0.0034	0.0008	0.0055	0.0001	0.028	0.307	0.555	0.526	0.877	1.04E-03	4.64E-04	2.91E-03	6.07E-05	-10.97	9.67
	63	0.0035	0.0008	0.0057	0.0001	0.029	0.303	0.550	0.521	0.876	1.07E-03	4.60E-04	2.98E-03	6.20E-05	-10.94	9.65
	126	0.0035	0.0007	0.0056	0.0001	0.028	0.306	0.553	0.524	0.877	1.07E-03	3.87E-04	2.91E-03	6.50E-05	-10.91	9.59
	216	0.0037	0.0006	0.0057	0.0001	0.029	0.303	0.550	0.521	0.876	1.11E-03	3.04E-04	2.96E-03	6.96E-05	-10.84	9.52
32-2	Feed	0.0011	0.0000	0.0017	0.0001	0.008	0.466	0.694	0.681	0.919	5.28E-04	1.33E-06	1.14E-03	6.66E-05	-11.30	9.25
	9	0.0005	0.0013	0.0017	0.0000	0.008	0.467	0.694	0.681	0.919	2.36E-04	9.31E-04	1.19E-03	2.36E-05	-12.18	10.25
	18	0.0005	0.0011	0.0016	0.0000	0.008	0.477	0.702	0.690	0.921	2.51E-04	7.77E-04	1.12E-03	2.48E-05	-12.16	10.22
	27	0.0006	0.0009	0.0016	0.0000	0.008	0.481	0.705	0.692	0.922	2.77E-04	6.67E-04	1.09E-03	2.78E-05	-12.07	10.11
	36	0.0006	0.0009	0.0016	0.0000	0.008	0.479	0.704	0.691	0.921	3.03E-04	6.20E-04	1.08E-03	2.85E-05	-12.06	10.12
	63	0.0008	0.0007	0.0016	0.0000	0.008	0.476	0.702	0.689	0.921	3.60E-04	4.58E-04	1.09E-03	3.42E-05	-11.89	9.95
	126	0.0008	0.0005	0.0016	0.0000	0.008	0.473	0.700	0.686	0.920	3.98E-04	3.58E-04	1.11E-03	3.75E-05	-11.81	9.88
	153	0.0009	0.0004	0.0016	0.0000	0.008	0.472	0.698	0.685	0.920	4.18E-04	3.05E-04	1.12E-03	3.92E-05	-11.76	9.84

Appendix B: Laboratory measurement of pH in experiments

Label	Time min	Time sec	t^1/2	Mass g	pH	H^+ mol/L	$\Delta(H_o-H_f)$ mol/L	Flow kg/sec	JH^+ mol/m^{2}sec
Experiment 1: 329 mg/L									
329-1-0	Feed				3.76	1.74E-04			
329-1-1	9	540	23.24	11.34	4.26	5.50E-05	1.19E-04	2.10E-05	5.55E-07
329-1-2	18	1080	32.86	11.16	4.20	6.31E-05	1.11E-04	2.07E-05	5.09E-07
329-1-3	27	1620	40.25	11.06	4.18	6.61E-05	1.08E-04	2.05E-05	4.91E-07
329-1-4	36	2160	46.48	11.10	4.14	7.24E-05	1.01E-04	2.06E-05	4.64E-07
329-1-5	45	2700	51.96	11.23	4.11	7.76E-05	9.62E-05	2.08E-05	4.45E-07
329-1-6	54	3240	56.92	11.00	4.10	7.94E-05	9.43E-05	2.04E-05	4.27E-07
329-1-7	63	3780	61.48	11.25	4.12	7.59E-05	9.79E-05	2.08E-05	4.54E-07
329-1-8	72	4320	65.73	11.39	4.12	7.59E-05	9.79E-05	2.11E-05	4.60E-07
329-1-9	81	4860	69.71	11.38	4.12	7.59E-05	9.79E-05	2.11E-05	4.59E-07
329-1-10	90	5400	73.48	11.35	4.07	8.51E-05	8.87E-05	2.10E-05	4.15E-07
329-1-11	99	5940	77.07	11.28	4.12	7.59E-05	9.79E-05	2.09E-05	4.55E-07
329-1-12	108	6480	80.50	11.27	4.09	8.13E-05	9.25E-05	2.09E-05	4.30E-07
329-1-13	117	7020	83.79	11.23	4.10	7.94E-05	9.43E-05	2.08E-05	4.37E-07
329-1-14	126	7560	86.95	10.35	4.07	8.51E-05	8.87E-05	1.92E-05	3.78E-07
329-1-15	135	8100	90.00	11.17	4.07	8.51E-05	8.87E-05	2.07E-05	4.08E-07
329-1-16	144	8640	92.95	10.90	4.07	8.51E-05	8.87E-05	2.02E-05	3.98E-07
329-1-17	153	9180	95.81	10.88	4.07	8.51E-05	8.87E-05	2.01E-05	3.97E-07
329-1-18	162	9720	98.59	10.90	4.06	8.71E-05	8.67E-05	2.02E-05	3.89E-07
329-1-19	171	10260	101.29	11.16	4.06	8.71E-05	8.67E-05	2.07E-05	3.99E-07
329-1-20	180	10800	103.92	11.19	4.06	8.71E-05	8.67E-05	2.07E-05	4.00E-07
329-1-21	189	11340	106.49	11.30	4.05	8.91E-05	8.47E-05	2.09E-05	3.94E-07
329-1-22	198	11880	109.00	10.84	4.06	8.71E-05	8.67E-05	2.01E-05	3.87E-07
329-1-23	207	12420	111.45	11.16	4.08	8.32E-05	9.06E-05	2.07E-05	4.17E-07
329-1-24	216	12960	113.84	11.12	4.07	8.51E-05	8.87E-05	2.06E-05	4.06E-07
329-1-25	225	13500	116.19	11.14	4.06	8.71E-05	8.67E-05	2.06E-05	3.98E-07
Experiment 2: 329 mg/L									
329-2-0	Feed				3.76	1.74E-04			
329-2-1	9	540	23.24	10.25	4.24	5.75E-05	1.16E-04	1.90E-05	4.91E-07
329-2-2	18	1080	32.86	10.51	4.18	6.61E-05	1.08E-04	1.95E-05	4.67E-07
329-2-3	27	1620	40.25	10.75	4.15	7.08E-05	1.03E-04	1.99E-05	4.56E-07
329-2-4	36	2160	46.48	10.70	4.14	7.24E-05	1.01E-04	1.98E-05	4.47E-07
329-2-5	45	2700	51.96	10.64	4.13	7.41E-05	9.96E-05	1.97E-05	4.37E-07
329-2-6	54	3240	56.92	11.15	4.12	7.59E-05	9.79E-05	2.06E-05	4.50E-07
329-2-7	63	3780	61.48	10.58	4.12	7.59E-05	9.79E-05	1.96E-05	4.27E-07
329-2-8	72	4320	65.73	10.52	4.10	7.94E-05	9.43E-05	1.95E-05	4.09E-07
329-2-9	81	4860	69.71	10.75	4.10	7.94E-05	9.43E-05	1.99E-05	4.18E-07
329-2-10	90	5400	73.48	10.75	4.09	8.13E-05	9.25E-05	1.99E-05	4.10E-07

329-2-11	99	5940	77.07	10.45	4.11	7.76E-05	9.62E-05	1.93E-05	4.14E-07
329-2-12	108	6480	80.50	10.72	4.09	8.13E-05	9.25E-05	1.98E-05	4.08E-07
329-2-13	117	7020	83.79	10.62	4.09	8.13E-05	9.25E-05	1.97E-05	4.05E-07
329-2-14	126	7560	86.95	10.68	4.08	8.32E-05	9.06E-05	1.98E-05	3.99E-07
329-2-15	135	8100	90.00	10.42	4.08	8.32E-05	9.06E-05	1.93E-05	3.89E-07
329-2-16	144	8640	92.95	10.58	4.09	8.13E-05	9.25E-05	1.96E-05	4.03E-07
329-2-17	153	9180	95.81	10.67	4.07	8.51E-05	8.87E-05	1.98E-05	3.90E-07
329-2-18	162	9720	98.59	10.62	4.08	8.32E-05	9.06E-05	1.97E-05	3.97E-07
329-2-19	171	10260	101.29	10.56	4.09	8.13E-05	9.25E-05	1.95E-05	4.02E-07
329-2-20	180	10800	103.92	10.62	4.08	8.32E-05	9.06E-05	1.97E-05	3.97E-07
329-2-21	189	11340	106.49	10.39	4.07	8.51E-05	8.87E-05	1.92E-05	3.80E-07
329-2-22	198	11880	109.00	10.56	4.06	8.71E-05	8.67E-05	1.96E-05	3.77E-07
329-2-23	207	12420	111.45	10.56	4.07	8.51E-05	8.87E-05	1.96E-05	3.86E-07
329-2-24	216	12960	113.84	10.39	4.09	8.13E-05	9.25E-05	1.92E-05	3.96E-07
329-2-25	225	13500	116.19	10.44	4.06	8.71E-05	8.67E-05	1.93E-05	3.73E-07
329-2-26	234	14040	118.49	10.32	4.08	8.32E-05	9.06E-05	1.91E-05	3.85E-07
329-2-27	243	14580	120.75	10.45	4.07	8.51E-05	8.87E-05	1.94E-05	3.82E-07
329-2-28	252	15120	122.96	10.39	4.06	8.71E-05	8.67E-05	1.92E-05	3.71E-07
329-2-29	261	15660	125.14	10.45	4.07	8.51E-05	8.87E-05	1.93E-05	3.82E-07
329-2-30	270	16200	127.28	10.44	4.07	8.51E-05	8.87E-05	1.93E-05	3.81E-07
Experiment 1: 162 mg/L									
162-1-0	Feed				3.93	1.17E-04			
162-1-1	9	540	23.24	9.67	4.29	5.13E-05	6.62E-05	1.79E-05	2.64E-07
162-1-2	18	1080	32.86	10.96	4.25	5.62E-05	6.13E-05	2.03E-05	2.77E-07
162-1-3	27	1620	40.25	10.07	4.21	6.17E-05	5.58E-05	1.86E-05	2.32E-07
162-1-4	36	2160	46.48	10.59	4.19	6.46E-05	5.29E-05	1.96E-05	2.31E-07
162-1-5	45	2700	51.96	10.56	4.18	6.61E-05	5.14E-05	1.95E-05	2.24E-07
162-1-6	54	3240	56.92	10.47	4.18	6.61E-05	5.14E-05	1.94E-05	2.22E-07
162-1-7	63	3780	61.48	10.63	4.17	6.76E-05	4.99E-05	1.97E-05	2.19E-07
162-1-8	72	4320	65.73	10.61	4.17	6.76E-05	4.99E-05	1.96E-05	2.18E-07
162-1-9	81	4860	69.71	10.60	4.16	6.92E-05	4.83E-05	1.96E-05	2.11E-07
162-1-10	90	5400	73.48	10.60	4.14	7.24E-05	4.50E-05	1.96E-05	1.97E-07
162-1-11	99	5940	77.07	10.64	4.15	7.08E-05	4.67E-05	1.97E-05	2.05E-07
162-1-12	108	6480	80.50	10.60	4.14	7.24E-05	4.50E-05	1.96E-05	1.97E-07
162-1-13	117	7020	83.79	10.51	4.14	7.24E-05	4.50E-05	1.95E-05	1.95E-07
162-1-14	126	7560	86.95	10.64	4.15	7.08E-05	4.67E-05	1.97E-05	2.05E-07
162-1-15	135	8100	90.00	10.92	4.16	6.92E-05	4.83E-05	2.02E-05	2.17E-07
162-1-16	144	8640	92.95	12.19	4.15	7.08E-05	4.67E-05	2.26E-05	2.34E-07
162-1-18	153	9180	95.81	10.68	4.13	7.41E-05	4.34E-05	1.98E-05	1.91E-07
162-1-19	162	9720	98.59	10.68	4.12	7.59E-05	4.16E-05	1.98E-05	1.83E-07
162-1-20	171	10260	101.29	10.73	4.11	7.76E-05	3.99E-05	1.99E-05	1.76E-07
162-1-21	180	10800	103.92	10.36	4.13	7.41E-05	4.34E-05	1.92E-05	1.85E-07
162-1-22	189	11340	106.49	10.54	4.12	7.59E-05	4.16E-05	1.95E-05	1.81E-07

162-1-23	198	11880	109.00	10.68	4.12	7.59E-05	4.16E-05	1.98E-05	1.83E-07
162-1-24	207	12420	111.45	10.69	4.11	7.76E-05	3.99E-05	1.98E-05	1.76E-07
162-1-25	216	12960	113.84	10.75	4.10	7.94E-05	3.81E-05	1.99E-05	1.69E-07
162-1-26	225	13500	116.19	10.62	4.11	7.76E-05	3.99E-05	1.97E-05	1.74E-07
162-1-27	234	14040	118.49	10.71	4.11	7.76E-05	3.99E-05	1.98E-05	1.76E-07
162-1-28	243	14580	120.75	10.65	4.10	7.94E-05	3.81E-05	1.97E-05	1.67E-07
162-1-29	252	15120	122.96	10.68	4.10	7.94E-05	3.81E-05	1.98E-05	1.67E-07
162-1-30	261	15660	125.14	10.68	4.10	7.94E-05	3.81E-05	1.98E-05	1.67E-07
Experiment 2: 162 mg/L									
162-2-0	feed				3.8	1.6E-04			
162-2-1	9	540	23.24	11.63	4.17	6.76E-05	9.09E-05	2.15E-05	4.35E-07
162-2-2	18	1080	32.86	11.46	4.13	7.41E-05	8.44E-05	2.12E-05	3.98E-07
162-2-3	27	1620	40.25	11.53	4.11	7.76E-05	8.09E-05	2.13E-05	3.84E-07
162-2-4	36	2160	46.48	11.48	4.11	7.76E-05	8.09E-05	2.13E-05	3.83E-07
162-2-5	45	2700	51.96	11.50	4.08	8.32E-05	7.53E-05	2.13E-05	3.57E-07
162-2-6	54	3240	56.92	10.83	4.09	8.13E-05	7.72E-05	2.01E-05	3.45E-07
162-2-7	63	3780	61.48	10.98	4.09	8.13E-05	7.72E-05	2.03E-05	3.49E-07
162-2-8	72	4320	65.73	10.89	4.08	8.32E-05	7.53E-05	2.02E-05	3.38E-07
162-2-9	81	4860	69.71	10.78	4.06	8.71E-05	7.14E-05	2.00E-05	3.17E-07
162-2-10	90	5400	73.48	10.82	4.08	8.32E-05	7.53E-05	2.00E-05	3.36E-07
162-2-11	99	5940	77.07	10.52	4.07	8.51E-05	7.34E-05	1.95E-05	3.18E-07
162-2-12	108	6480	80.50	10.64	4.08	8.32E-05	7.53E-05	1.97E-05	3.30E-07
162-2-13	117	7020	83.79	10.72	4.08	8.32E-05	7.53E-05	1.98E-05	3.33E-07
162-2-14	126	7560	86.95	10.70	4.05	8.91E-05	6.94E-05	1.98E-05	3.06E-07
162-2-15	135	8100	90.00	10.58	4.04	9.12E-05	6.73E-05	1.96E-05	2.93E-07
162-2-16	144	8640	92.95	10.44	4.07	8.51E-05	7.34E-05	1.93E-05	3.16E-07
162-2-17	153	9180	95.81	10.67	4.07	8.51E-05	7.34E-05	1.98E-05	3.22E-07
162-2-18	162	9720	98.59	10.60	4.07	8.51E-05	7.34E-05	1.96E-05	3.20E-07
162-2-19	171	10260	101.29	10.58	4.07	8.51E-05	7.34E-05	1.96E-05	3.20E-07
162-2-20	180	10800	103.92	10.92	4.05	8.91E-05	6.94E-05	2.02E-05	3.12E-07
162-2-21	189	11340	106.49	10.33	4.05	8.91E-05	6.94E-05	1.91E-05	2.95E-07
162-2-22	198	11880	109.00	10.56	4.06	8.71E-05	7.14E-05	1.96E-05	3.11E-07
162-2-23	207	12420	111.45	10.63	4.05	8.91E-05	6.94E-05	1.97E-05	3.04E-07
162-2-24	216	12960	113.84	10.99	4.06	8.71E-05	7.14E-05	2.04E-05	3.23E-07
162-2-25	225	13500	116.19	10.56	4.05	8.91E-05	6.94E-05	1.96E-05	3.02E-07
Experiment 1: 108 mg/L									
108-1-0	Feed				3.93	1.17E-04			
108-1-1	9	540	24.49	11.02	4.27	5.37E-05	6.38E-05	2.04E-05	2.90E-07
108-1-2	18	1080	33.76	10.73	4.23	5.89E-05	5.86E-05	1.99E-05	2.59E-07
108-1-3	27	1620	40.99	10.78	4.19	6.46E-05	5.29E-05	2.00E-05	2.35E-07
108-1-4	36	2160	47.12	10.87	4.16	6.92E-05	4.83E-05	2.01E-05	2.16E-07
108-1-5	45	2700	52.54	10.75	4.14	7.24E-05	4.50E-05	1.99E-05	2.00E-07
108-1-6	54	3240	57.45	10.79	4.15	7.08E-05	4.67E-05	2.00E-05	2.08E-07

108-1-7	63	3780	61.97	10.85	4.15	7.08E-05	4.67E-05	2.01E-05	2.09E-07
108-1-8	72	4320	66.18	10.80	4.15	7.08E-05	4.67E-05	2.00E-05	2.08E-07
108-1-9	81	4860	70.14	10.83	4.13	7.41E-05	4.34E-05	2.01E-05	1.93E-07
108-1-10	90	5400	73.89	10.59	4.15	7.08E-05	4.67E-05	1.96E-05	2.04E-07
108-1-11	99	5940	77.46	10.21	4.15	7.08E-05	4.67E-05	1.89E-05	1.96E-07
108-1-12	108	6480	80.87	10.76	4.14	7.24E-05	4.50E-05	1.99E-05	2.00E-07
108-1-13	117	7020	84.14	10.71	4.15	7.08E-05	4.67E-05	1.98E-05	2.06E-07
108-1-14	126	7560	87.29	10.75	4.13	7.41E-05	4.34E-05	1.99E-05	1.92E-07
108-1-15	135	8100	90.33	10.57	4.13	7.41E-05	4.34E-05	1.96E-05	1.89E-07
108-1-16	144	8640	93.27	10.77	4.15	7.08E-05	4.67E-05	1.99E-05	2.07E-07
108-1-17	153	9180	96.12	10.75	4.12	7.59E-05	4.16E-05	1.99E-05	1.84E-07
108-1-18	162	9720	98.89	10.83	4.11	7.76E-05	3.99E-05	2.00E-05	1.78E-07
108-1-19	171	10260	101.59	10.81	4.12	7.59E-05	4.16E-05	2.00E-05	1.86E-07
108-1-20	180	10800	104.21	10.77	4.12	7.59E-05	4.16E-05	1.99E-05	1.85E-07
108-1-21	189	11340	106.77	10.80	4.12	7.59E-05	4.16E-05	2.00E-05	1.85E-07
108-1-22	198	11880	109.27	10.76	4.10	7.94E-05	3.81E-05	1.99E-05	1.69E-07
108-1-23	207	12420	111.71	10.77	4.10	7.94E-05	3.81E-05	1.99E-05	1.69E-07
108-1-24	216	12960	114.11	10.62	4.10	7.94E-05	3.81E-05	1.97E-05	1.67E-07
Experiment 2: 108 mg/L									
108-2-0	Feed				3.98	1.05E-04			
108-2-1	9	540	24.49	10.79	4.54	2.88E-05	7.59E-05	2.00E-05	3.37E-07
108-2-2	18	1080	33.76	10.90	4.46	3.47E-05	7.00E-05	2.02E-05	3.15E-07
108-2-3	27	1620	40.99	10.89	4.39	4.07E-05	6.40E-05	2.02E-05	2.87E-07
108-2-4	36	2160	47.12	10.99	4.35	4.47E-05	6.00E-05	2.03E-05	2.72E-07
108-2-5	45	2700	52.65	11.52	4.31	4.90E-05	5.57E-05	2.13E-05	2.65E-07
108-2-6	54	3240	57.65	11.59	4.29	5.13E-05	5.34E-05	2.15E-05	2.55E-07
108-2-7	63	3780	62.16	11.26	4.28	5.25E-05	5.22E-05	2.09E-05	2.42E-07
108-2-8	72	4320	66.36	11.25	4.30	5.01E-05	5.46E-05	2.08E-05	2.53E-07
108-2-9	81	4860	70.31	11.27	4.28	5.25E-05	5.22E-05	2.09E-05	2.43E-07
108-2-10	90	5400	74.05	11.16	4.25	5.62E-05	4.85E-05	2.07E-05	2.23E-07
108-2-11	99	5940	77.61	11.06	4.27	5.37E-05	5.10E-05	2.05E-05	2.32E-07
108-2-12	108	6480	81.02	11.22	4.26	5.50E-05	4.98E-05	2.08E-05	2.30E-07
108-2-13	117	7020	84.29	11.12	4.25	5.62E-05	4.85E-05	2.06E-05	2.22E-07
108-2-14	126	7560	87.43	11.07	4.25	5.62E-05	4.85E-05	2.05E-05	2.21E-07
108-2-15	135	8100	90.47	11.05	4.25	5.62E-05	4.85E-05	2.05E-05	2.21E-07
108-2-16	144	8640	93.40	10.77	4.25	5.62E-05	4.85E-05	1.99E-05	2.15E-07
108-2-17	153	9180	96.25	10.75	4.24	5.75E-05	4.72E-05	1.99E-05	2.09E-07
108-2-18	162	9720	99.02	10.83	4.23	5.89E-05	4.58E-05	2.00E-05	2.04E-07
108-2-19	171	10260	101.71	11.10	4.22	6.03E-05	4.45E-05	2.05E-05	2.03E-07
108-2-20	180	10800	104.33	11.04	4.23	5.89E-05	4.58E-05	2.04E-05	2.08E-07
108-2-21	189	11340	106.88	11.10	4.23	5.89E-05	4.58E-05	2.06E-05	2.10E-07
108-2-22	198	11880	109.38	11.09	4.23	5.89E-05	4.58E-05	2.05E-05	2.09E-07
108-2-23	207	12420	111.82	11.11	4.22	6.03E-05	4.45E-05	2.06E-05	2.04E-07

108-2-24	216	12960	114.21	11.02	4.23	5.89E-05	4.58E-05	2.04E-05	2.08E-07
108-2-25	225	13500	116.19	9.34	4.22	6.03E-05	4.45E-05	1.73E-05	1.71E-07
Experiment 1: 32 mg/L									
32-1-0	Feed				4.16	6.91831E-05			
32-1-1	9	540	23.24	23.24	4.48	3.31E-05	3.61E-05	4.30E-05	3.45E-07
32-1-2	18	1080	32.86	32.86	4.48	3.31E-05	3.61E-05	6.09E-05	4.88E-07
32-1-3	27	1620	40.25	40.25	4.48	3.31E-05	3.61E-05	7.45E-05	5.98E-07
32-1-4	36	2160	46.48	46.48	4.47	3.39E-05	3.53E-05	8.61E-05	6.76E-07
32-1-5	45	2700	51.96	51.96	4.43	3.72E-05	3.20E-05	9.62E-05	6.86E-07
32-1-6	54	3240	56.92	56.92	4.42	3.80E-05	3.12E-05	1.05E-04	7.31E-07
32-1-7	63	3780	61.48	61.48	4.40	3.98E-05	2.94E-05	1.14E-04	7.44E-07
32-1-8	72	4320	65.73	65.73	4.40	3.98E-05	2.94E-05	1.22E-04	7.96E-07
32-1-9	81	4860	69.71	69.71	4.42	3.80E-05	3.12E-05	1.29E-04	8.95E-07
32-1-10	90	5400	73.48	73.48	4.40	3.98E-05	2.94E-05	1.36E-04	8.89E-07
32-1-11	99	5940	77.07	77.07	4.42	3.80E-05	3.12E-05	1.43E-04	9.90E-07
32-1-12	639	38340	195.81	195.81	4.40	3.98E-05	2.94E-05	3.63E-04	2.37E-06
Experiment 2: 32 mg/L									
32-2-0	Feed				4.14	7.24436E-05			
32-2-1	9	540	23.24	12.04	4.59	2.57E-05	4.67E-05	2.23E-05	2.32E-07
32-2-2	18	1080	32.86	11.86	4.57	2.69E-05	4.55E-05	2.20E-05	2.23E-07
32-2-3	27	1620	40.25	11.84	4.52	3.02E-05	4.22E-05	2.19E-05	2.06E-07
32-2-4	36	2160	46.48	11.94	4.51	3.09E-05	4.15E-05	2.21E-05	2.04E-07
32-2-5	45	2700	51.96	12.00	4.48	3.31E-05	3.93E-05	2.22E-05	1.95E-07
32-2-6	54	3240	56.92	12.00	4.45	3.55E-05	3.70E-05	2.22E-05	1.83E-07
32-2-7	63	3780	61.48	11.96	4.43	3.72E-05	3.53E-05	2.21E-05	1.74E-07
32-2-8	72	4320	65.73	11.53	4.43	3.72E-05	3.53E-05	2.14E-05	1.68E-07
32-2-9	81	4860	69.71	11.96	4.41	3.89E-05	3.35E-05	2.22E-05	1.65E-07
32-2-10	90	5400	73.48	11.92	4.40	3.98E-05	3.26E-05	2.21E-05	1.60E-07
32-2-11	99	5940	77.07	11.67	4.42	3.80E-05	3.44E-05	2.16E-05	1.66E-07
32-2-12	108	6480	80.50	10.97	4.42	3.80E-05	3.44E-05	2.03E-05	1.56E-07
32-2-13	117	7020	83.79	11.86	4.41	3.89E-05	3.35E-05	2.20E-05	1.64E-07
32-2-14	126	7560	86.95	11.76	4.39	4.07E-05	3.17E-05	2.18E-05	1.54E-07
32-2-15	135	8100	90.00	11.95	4.40	3.98E-05	3.26E-05	2.21E-05	1.61E-07
32-2-16	144	8640	92.95	9.85	4.38	4.17E-05	3.08E-05	1.82E-05	1.25E-07
32-2-17	153	9180	95.81	10.77	4.37	4.27E-05	2.98E-05	2.00E-05	1.32E-07
32-2-18	162	9720	98.59	11.99	4.36	4.37E-05	2.88E-05	2.22E-05	1.42E-07
32-2-19	171	10260	101.29	10.52	4.37	4.27E-05	2.98E-05	1.95E-05	1.29E-07
32-2-20	180	10800	103.92	11.60	4.37	4.27E-05	2.98E-05	2.15E-05	1.42E-07

Appendix C: Chemical analyses of effluent solution in the MFR experiment

Solution Al mg/L	t sec	Mass g	Al^{3+} mg/L	Ca^{2+} mg/L	S mg/L	pH	Flow (kg/sec)	Al^{3+} mol/kg	Ca^{2+} mol/kg	S mol/kg	H^{+} mol/kg
329-1	0	feed	304.81	0.09	539.07	3.76		1.13E-02	2.17E-06	1.68E-02	1.74E-04
	540	11.34	170.90	357.20	508.60	4.26	2.10E-05	6.33E-03	8.91E-03	1.59E-02	5.50E-05
	1080	11.16	196.80	300.10	508.90	4.20	2.07E-05	7.29E-03	7.49E-03	1.59E-02	6.31E-05
	1620	11.06	217.30	251.40	514.60	4.18	2.05E-05	8.05E-03	6.27E-03	1.60E-02	6.61E-05
	2160	11.10	233.60	207.80	512.20	4.14	2.06E-05	8.66E-03	5.18E-03	1.60E-02	7.24E-05
	3780	11.25	264.15	162.16	532.41	4.12	2.08E-05	9.79E-03	4.05E-03	1.66E-02	7.59E-05
	7560	10.35	279.13	117.10	533.55	4.07	1.92E-05	1.03E-02	2.92E-03	1.66E-02	8.51E-05
	12960	11.12	284.01	95.92	530.20	4.06	2.06E-05	1.05E-02	2.39E-03	1.65E-02	8.71E-05
162-1	0	feed	150.82	0.07	266.51	3.93		5.59E-03	1.72E-06	8.31E-03	1.17E-04
	540	10.12	91.80	139.70	249.00	4.29	1.87E-05	3.40E-03	3.49E-03	7.77E-03	5.13E-05
	1080	10.96	108.70	106.40	256.00	4.25	2.03E-05	4.03E-03	2.65E-03	7.98E-03	5.62E-05
	1620	10.07	119.10	83.80	257.60	4.21	1.86E-05	4.41E-03	2.09E-03	8.03E-03	6.17E-05
	2160	10.59	127.00	72.50	261.50	4.19	1.96E-05	4.71E-03	1.81E-03	8.16E-03	6.46E-05
	3780	10.63	130.90	54.29	259.85	4.17	1.97E-05	4.85E-03	1.35E-03	8.10E-03	6.76E-05
	7560	10.64	135.05	43.44	261.16	4.15	1.97E-05	5.01E-03	1.08E-03	8.15E-03	7.08E-05
	12960	10.75	139.50	35.79	264.37	4.11	1.99E-05	5.17E-03	8.93E-04	8.25E-03	7.76E-05
108-1	0	feed	107.90	0.00	192.40	3.93		4.00E-03	0.00E+00	6.00E-03	1.17E-04
	540	11.02	79.50	70.50	176.30	4.27	2.04E-05	2.95E-03	1.76E-03	5.50E-03	5.37E-05
	1080	10.73	84.50	50.63	175.50	4.23	1.99E-05	3.13E-03	1.26E-03	5.47E-03	5.89E-05
	1620	10.78	89.00	39.60	178.20	4.19	2.00E-05	3.30E-03	9.88E-04	5.56E-03	6.46E-05
	2160	10.87	91.10	33.50	177.20	4.16	2.01E-05	3.38E-03	8.36E-04	5.53E-03	6.92E-05
	3780	10.85	95.53	33.53	183.29	4.15	2.01E-05	3.54E-03	8.37E-04	5.72E-03	7.08E-05
	7560	10.75	94.85	28.05	177.90	4.13	1.99E-05	3.52E-03	7.00E-04	5.55E-03	7.41E-05
	12960	10.62	98.95	22.14	181.64	4.10	1.97E-05	3.67E-03	5.52E-04	5.66E-03	7.94E-05
32-2	0	feed	30.54	0.08	53.45	4.14		1.13E-03	1.92E-06	1.67E-03	7.24E-05
	540	12.04	13.62	53.76	55.85	4.59	2.23E-05	5.05E-04	1.34E-03	1.74E-03	2.57E-05
	1080	11.86	14.22	44.37	52.06	4.57	2.20E-05	5.27E-04	1.11E-03	1.62E-03	2.69E-05
	1620	11.84	15.56	37.95	50.50	4.52	2.19E-05	5.76E-04	9.47E-04	1.57E-03	3.02E-05
	2160	11.94	17.06	35.33	50.08	4.51	2.21E-05	6.32E-04	8.81E-04	1.56E-03	3.09E-05
	3780	11.96	20.40	26.19	50.73	4.43	2.21E-05	7.56E-04	6.53E-04	1.58E-03	3.72E-05
	7560	11.76	22.68	20.53	51.74	4.39	2.18E-05	8.40E-04	5.12E-04	1.61E-03	4.07E-05
	9180	10.77	23.92	17.52	52.49	4.37	1.99E-05	8.87E-04	4.37E-04	1.64E-03	4.27E-05

Appendix D: Reproducibility of pH for two independent experiments

A. Table of pH for two independent experiments for each concentration

Time (min)	**329-1**	**329-2**	**162-1**	**162-2**	**108-1**	**108-2**	**32-1**	**32-2**
Feed	3.76	3.76	3.93	3.8	3.93	3.98	4.16	4.14
9	4.26	4.24	4.29	4.17	4.27	4.54	4.48	4.59
18	4.20	4.18	4.25	4.13	4.23	4.46	4.48	4.57
27	4.18	4.15	4.21	4.11	4.19	4.39	4.48	4.52
36	4.14	4.14	4.19	4.11	4.16	4.35	4.47	4.51
45	4.11	4.13	4.18	4.08	4.14	4.31	4.43	4.48
54	4.10	4.12	4.18	4.09	4.15	4.29	4.42	4.45
63	4.12	4.12	4.17	4.09	4.15	4.28	4.40	4.43
72	4.12	4.10	4.17	4.08	4.15	4.30	4.40	4.43
81	4.12	4.10	4.16	4.06	4.13	4.28	4.42	4.41
90	4.07	4.09	4.14	4.08	4.15	4.25	4.40	4.40
99	4.12	4.11	4.15	4.07	4.15	4.27	4.42	4.42
108	4.09	4.09	4.14	4.08	4.14	4.26		4.42
117	4.10	4.09	4.14	4.08	4.15	4.25		4.41
126	4.07	4.08	4.15	4.05	4.13	4.25		4.39
135	4.07	4.08	4.16	4.04	4.13	4.25		4.40
144	4.07	4.09	4.15	4.07	4.15	4.25		4.38
153	4.07	4.07	4.13	4.07	4.12	4.24		4.37
162	4.06	4.08	4.12	4.07	4.11	4.23		4.36
171	4.06	4.09	4.11	4.07	4.12	4.22		4.37
180	4.06	4.08	4.13	4.05	4.12	4.23		4.37
189	4.05	4.07	4.12	4.05	4.12	4.23		
198	4.06	4.06	4.12	4.06	4.10	4.23		
207	4.08	4.07	4.11	4.05	4.10	4.22		
216	4.07	4.09	4.10	4.06	4.10	4.23		
225	4.06	4.06	4.11	4.05				
234		4.08	4.11					
243		4.07	4.10					
252		4.06	4.10					
261		4.07	4.10					
270		4.07						

B. Graph of pH vs time of two independent experiments for 329 mg/L Al

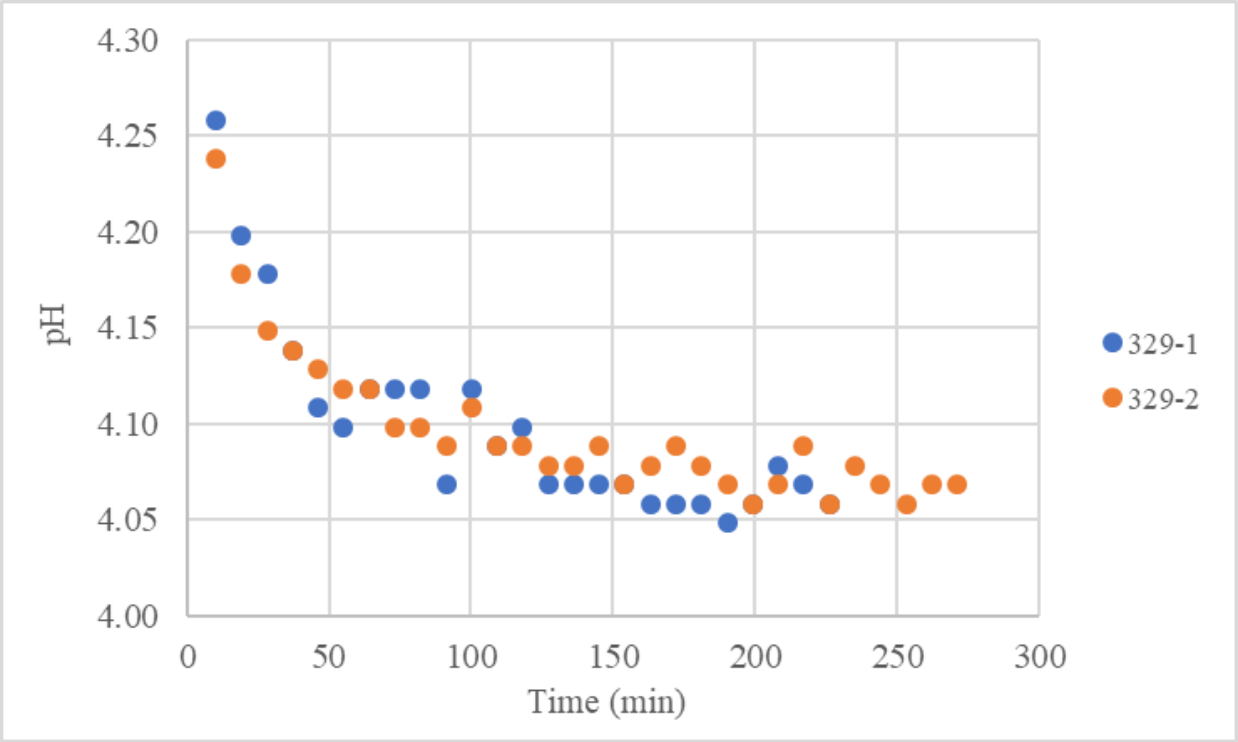

Appendix E: Duplicate analyses of the same solutions

Sample	Time sec	Al mg/L	Ca mg/L	S mg/L	Al repeated mg/L	Ca repeated mg/L	S repeated mg/L	Difference Al %	Difference Ca %	Difference S %
Detection Limit mg/L		**0.036**	**0.033**	**0.055**	**0.036**	**0.033**	**0.055**			
32-2-1	540	13.616	53.763	55.845	12.922	53.612	55.182	5.10	0.28	1.19
108-1-7	3780	95.534	33.532	183.289	95.076	34.282	181.847	0.48	-2.24	0.79
108-1-14	7560	94.849	28.045	177.896	94.644	27.651	176.66	0.22	1.40	0.69
108-1-24	12960	98.946	22.141	181.641	98.888	21.533	179.879	0.06	2.75	0.97

Appendix F: SEM coating figures from batch reactor experiment

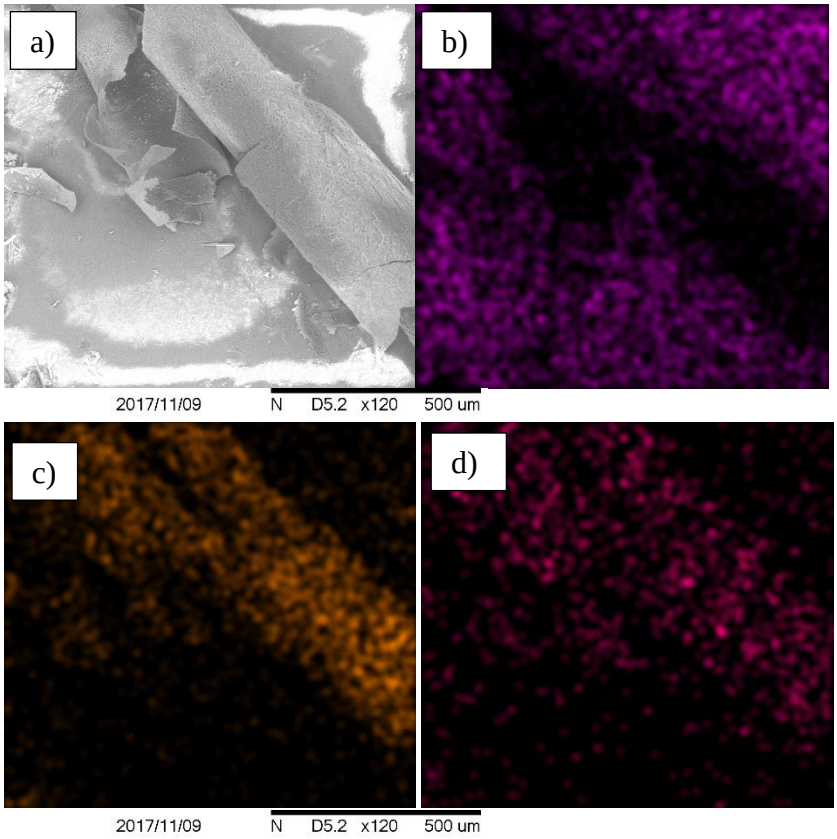

SEM back-scatter image of coating the 108 mg/L Al experiment. Concentrations maps of b) calcium c) aluminum and d) sulfur. Maps are of the same field of view. Brighter colors in the Ca, Al and S maps reflect higher concentrations.

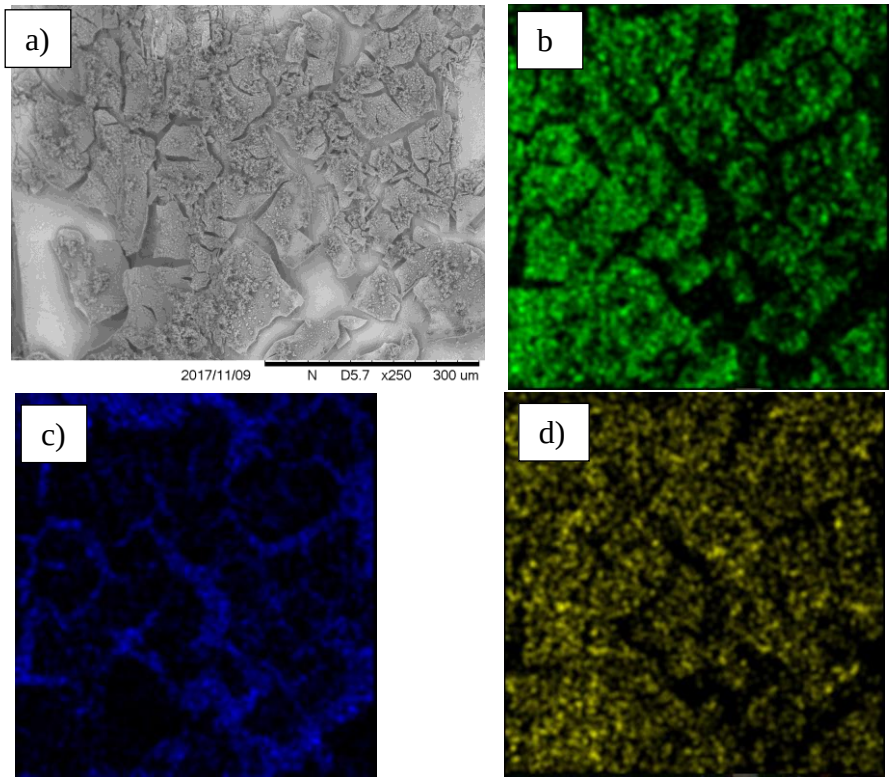

SEM back-scatter image of coating the 108 mg/L Al experiment. Concentrations maps of b) aluminum c) calcium and d) sulfur. Maps are of the same field of view. Brighter colors in the Ca, Al and S maps reflect higher concentrations.

Appendix G: XRD patterns from batch reactor experiments

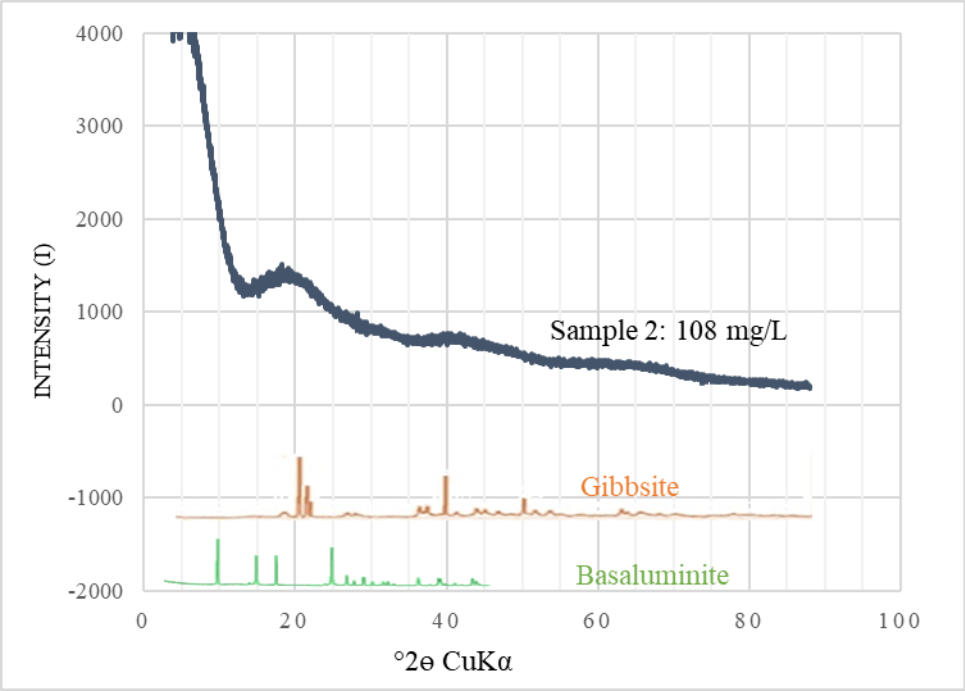

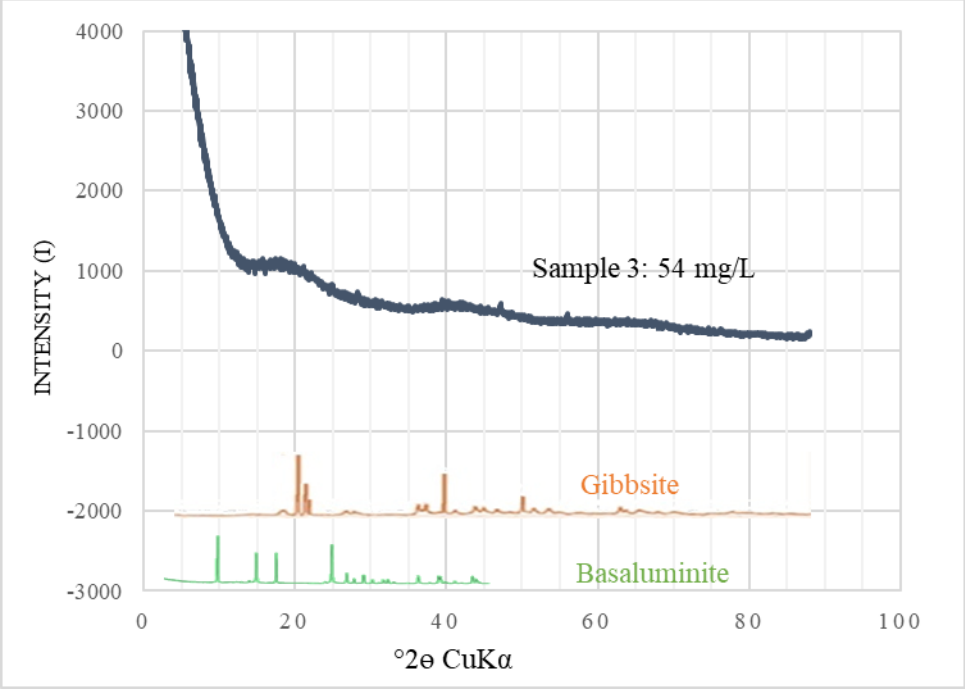

Appendix H: Diffusion coefficient calculations

Solution Al mg/L	**t sec**	**J(Al) mol/m²sec**	**J(Ca) mol/m²sec**	**J(S) mol/m²sec**	**J(H) mol/m²sec**	**J(cal) mol/m²sec**	**J(bas) mol/m²sec**	**J(gib) mol/m²sec**	**J(Alout) mol/m²sec**	**J(H)/ J(cal)**
329-1	540	-2.32E-05	4.16E-05	-4.44E-06	-5.55E-07	-8.32E-05	4.44E-05	1.63E-05	2.31E-05	0.007
	1080	-1.84E-05	3.44E-05	-4.33E-06	-5.09E-07	-6.88E-05	4.33E-05	3.31E-06	2.28E-05	0.007
	1620	-1.48E-05	2.86E-05	-3.48E-06	-4.91E-07	-5.72E-05	3.48E-05	2.62E-06	2.03E-05	0.009
	2160	-1.21E-05	2.37E-05	-3.83E-06	-4.64E-07	-4.74E-05	3.83E-05	-9.77E-06	1.93E-05	0.010
	3780	-6.99E-06	1.87E-05	-9.62E-07	-4.54E-07	-3.75E-05	9.62E-06	9.42E-06	1.89E-05	0.012
	7560	-4.06E-06	1.25E-05	-7.34E-07	-3.78E-07	-2.49E-05	7.34E-06	3.37E-06	1.46E-05	0.015
	12960	-3.53E-06	1.10E-05	-1.27E-06	-3.97E-07	-2.19E-05	1.27E-05	-4.61E-06	1.42E-05	0.018
162-1	540	-9.12E-06	1.45E-05	-2.28E-06	-2.76E-07	-2.91E-05	2.28E-05	3.44E-08	6.52E-06	0.010
	1080	-7.05E-06	1.20E-05	-1.48E-06	-2.77E-07	-2.40E-05	1.48E-05	3.38E-06	6.05E-06	0.012
	1620	-4.88E-06	8.67E-06	-1.15E-06	-2.32E-07	-1.73E-05	1.15E-05	7.94E-07	5.24E-06	0.013
	2160	-3.85E-06	7.88E-06	-6.82E-07	-2.31E-07	-1.58E-05	6.82E-06	3.37E-06	5.81E-06	0.015
	3780	-3.24E-06	5.93E-06	-9.11E-07	-2.19E-07	-1.19E-05	9.11E-06	-1.22E-06	4.19E-06	0.018
	7560	-2.56E-06	4.74E-06	-7.31E-07	-2.05E-07	-9.48E-06	7.31E-06	-1.09E-06	3.47E-06	0.022
	12960	-1.86E-06	3.95E-06	-2.96E-07	-1.77E-07	-7.89E-06	2.96E-06	2.03E-06	3.08E-06	0.022
108-1	540	-4.78E-06	7.99E-06	-2.28E-06	-2.90E-07	-1.60E-05	2.28E-05	-1.30E-05	6.49E-06	0.018
	1080	-3.83E-06	5.58E-06	-2.33E-06	-2.59E-07	-1.12E-05	2.33E-05	-1.65E-05	4.59E-06	0.023
	1620	-3.11E-06	4.39E-06	-1.97E-06	-2.35E-07	-8.78E-06	1.97E-05	-1.43E-05	3.61E-06	0.027
	2160	-2.79E-06	3.74E-06	-2.12E-06	-2.16E-07	-7.49E-06	2.12E-05	-1.71E-05	3.58E-06	0.029
	3780	-2.05E-06	3.74E-06	-1.27E-06	-2.09E-07	-7.48E-06	1.27E-05	-9.10E-06	4.09E-06	0.028
	7560	-2.14E-06	3.10E-06	-2.00E-06	-1.92E-07	-6.20E-06	2.00E-05	-1.76E-05	3.97E-06	0.031
	12960	-1.45E-06	2.42E-06	-1.47E-06	-1.67E-07	-4.84E-06	1.47E-05	-1.33E-05	3.58E-06	0.034
32-2	540	-3.11E-06	6.65E-06	3.70E-07	-2.32E-07	-1.33E-05	-3.70E-06	1.38E-05	3.45E-06	0.017
	1080	-2.96E-06	5.40E-06	-2.12E-07	-2.23E-07	-1.08E-05	2.12E-06	6.33E-06	2.58E-06	0.021
	1620	-2.71E-06	4.61E-06	-4.50E-07	-2.06E-07	-9.22E-06	4.50E-06	2.74E-06	2.20E-06	0.022
	2160	-2.46E-06	4.33E-06	-5.17E-07	-2.04E-07	-8.66E-06	5.17E-06	1.16E-06	2.52E-06	0.024
	3780	-1.85E-06	3.21E-06	-4.18E-07	-1.74E-07	-6.42E-06	4.18E-06	5.37E-07	1.88E-06	0.027
	7560	-1.41E-06	2.47E-06	-2.59E-07	-1.54E-07	-4.95E-06	2.59E-06	1.12E-06	1.38E-06	0.031
	9180	-1.09E-06	1.93E-06	-1.34E-07	-1.32E-07	-3.86E-06	1.34E-06	1.66E-06	9.97E-07	0.034

Solution Al mg/L	t sec	J(bas)/J(cal)	J(gib)/J(cal)	J(Alout)/J(cal)	J(Al) mol/m^{2}sec	J(-H) mol/m^{2}sec	n(Al) mol	x(bas) m	x(gib) m	cH mol/m^3	logD (bas)	logD (gib)
329-1	0				2.32E-05							
	540	0.534	0.196	-0.278	2.32E-05	1.66E-04	0.013	1.32E-06	8.02E-07	54.95	-11.40	-11.61
	1080	0.629	0.048	-0.331	1.84E-05	1.38E-04	0.024	2.50E-06	1.52E-06	63.10	-11.26	-11.48
	1620	0.608	0.046	-0.355	1.48E-05	1.14E-04	0.033	3.44E-06	2.09E-06	66.07	-11.22	-11.44
	2160	0.808	-0.206	-0.407	1.21E-05	9.48E-05	0.040	4.21E-06	2.56E-06	72.44	-11.26	-11.48
	3780	0.257	0.251	-0.504	6.99E-06	7.50E-05	0.055	5.83E-06	3.55E-06	75.86	-11.24	-11.45
	7560	0.295	0.135	-0.586	4.06E-06	4.98E-05	0.076	8.03E-06	4.89E-06	85.11	-11.33	-11.54
	12960	0.580	-0.211	-0.648	3.53E-06	4.38E-05	0.097	1.02E-05	6.20E-06	87.10	-11.29	-11.51
162-1	0				9.12E-06							
	540	0.784	0.001	-0.224	9.12E-06	5.82E-05	0.005	5.18E-07	3.15E-07	51.29	-12.23	-12.45
	1080	0.617	0.141	-0.252	7.05E-06	4.80E-05	0.009	9.77E-07	5.95E-07	56.23	-12.08	-12.29
	1620	0.665	0.046	-0.303	4.88E-06	3.46E-05	0.013	1.32E-06	8.01E-07	61.66	-12.13	-12.35
	2160	0.432	0.213	-0.368	3.85E-06	3.16E-05	0.015	1.56E-06	9.52E-07	64.57	-12.12	-12.33
	3780	0.766	-0.103	-0.352	3.24E-06	2.38E-05	0.021	2.17E-06	1.32E-06	67.61	-12.12	-12.33
	7560	0.771	-0.115	-0.366	2.56E-06	1.90E-05	0.032	3.32E-06	2.02E-06	70.79	-12.05	-12.27
	12960	0.375	0.257	-0.390	1.86E-06	1.58E-05	0.044	4.58E-06	2.78E-06	77.62	-12.03	-12.25
108-1	0				4.78E-06							
	540	1.425	-0.813	-0.406	4.78E-06	3.20E-05	0.003	2.72E-07	1.65E-07	53.70	-12.79	-13.01
	1080	2.080	-1.473	-0.410	3.83E-06	2.24E-05	0.005	5.16E-07	3.14E-07	58.88	-12.71	-12.92
	1620	2.244	-1.629	-0.411	3.11E-06	1.76E-05	0.007	7.13E-07	4.34E-07	64.57	-12.71	-12.93
	2160	2.830	-2.283	-0.478	2.79E-06	1.50E-05	0.008	8.81E-07	5.36E-07	69.18	-12.72	-12.94
	3780	1.698	-1.217	-0.547	2.05E-06	1.50E-05	0.012	1.29E-06	7.87E-07	70.79	-12.56	-12.78
	7560	3.226	-2.839	-0.640	2.14E-06	1.24E-05	0.020	2.13E-06	1.29E-06	74.13	-12.45	-12.66
	12960	3.037	-2.748	-0.740	1.45E-06	9.68E-06	0.030	3.15E-06	1.91E-06	79.43	-12.42	-12.63
32-2	0				3.11E-06							
	540	-0.278	1.038	-0.259	3.11E-06	2.66E-05	0.002	1.77E-07	1.07E-07	25.70	-12.74	-12.95
	1080	0.196	0.586	-0.239	2.96E-06	2.16E-05	0.003	3.49E-07	2.12E-07	26.92	-12.55	-12.77
	1620	0.488	0.297	-0.239	2.71E-06	1.84E-05	0.005	5.10E-07	3.10E-07	30.20	-12.51	-12.72
	2160	0.597	0.134	-0.291	2.46E-06	1.73E-05	0.006	6.57E-07	4.00E-07	30.90	-12.43	-12.65
	3780	0.651	0.084	-0.293	1.85E-06	1.28E-05	0.010	1.02E-06	6.23E-07	37.15	-12.45	-12.67
	7560	0.523	0.226	-0.279	1.41E-06	9.90E-06	0.016	1.67E-06	1.02E-06	40.74	-12.39	-12.61
	9180	0.347	0.430	-0.258	1.09E-06	7.72E-06	0.018	1.89E-06	1.15E-06	42.66	-12.47	-12.68

Appendix I: Figure of the mixed flow reactor experiment